

Principles and demonstrations of quantum information processing by NMR spectroscopy*

T. F. Havel¹, S. S. Somaroo¹, C.-H. Tseng² and D. G. Cory³

¹ BCMP, Harvard Medical School, Boston, MA 02115

² Harvard-Smithsonian Center for Astrophysics, Cambridge, MA 02138

³ Nuclear Engineering, MIT, Cambridge, MA 02139

Abstract. This paper surveys our recent research on quantum information processing by nuclear magnetic resonance (NMR) spectroscopy. We begin with a geometric introduction to the NMR of an ensemble of indistinguishable spins, and then show how this geometric interpretation is contained within an algebra of multispin product operators. This algebra is used throughout the rest of the paper to demonstrate that it provides a facile framework within which to study quantum information processing more generally. The implementation of quantum algorithms by NMR depends upon the availability of special kinds of mixed states, called pseudo-pure states, and we consider a number of different methods for preparing these states, along with analyses of how they scale with the number of spins. The quantum-mechanical nature of processes involving such macroscopic pseudo-pure states also is a matter of debate, and in order to discuss this issue in concrete terms we present the results of NMR experiments which constitute a macroscopic analogue Hardy's paradox. Finally, a detailed product operator description is given of recent NMR experiments which demonstrate a three-bit quantum error correcting code, using field gradients to implement a precisely-known decoherence model.

* Portions of this survey were presented at the AeroSense Workshop on Photonic Quantum Computing II, held in Orlando, Florida on April 16, 1998, at the Dagstuhl Seminar on Quantum Algorithms, held in Schloss Dagstuhl, Germany on May 10 – 15, 1998, and at the Workshop on Quantum Information, Decoherence and Chaos, held on Heron Island, Australia September 21 – 25, 1998; this paper is an updated and extended version of one published in the proceedings of the AeroSense meeting, available as vol. 3385 from the International Society for Optical Engineering, 1000 20th St., Bellingham, WA 98225, USA.

1 Introduction

It has recently proven possible to perform simple quantum computations by liquid-state NMR spectroscopy [12, 13, 14, 15, 16, 22, 32, 42]. This unprecedented level of coherent control promises to be quite useful not only in demonstrating the validity of many of the basic ideas behind quantum information processing, but more importantly, in providing researchers in the field with new physical insights and concrete problems to study. This is particularly true since the ensemble nature of the systems used for NMR computing differs substantially from the systems previously considered as candidate quantum computers. The use of ensembles provides tremendous redundancy, which makes computation with them relatively resistant to errors. It also has the potential to provide access to a limited form of massive classical parallelism [14], which could for example be used to speed up searches with Grover's algorithm by a constant but very large factor [9, 24, 36]. The barriers that have been encountered in extending NMR computing to nontrivial problems further raise interesting questions regarding the relations between microscopic and macroscopic order, and between the quantum and classical worlds [23, 43].

NMR computing is also contributing to quantum information processing through the assimilation of theoretical and experimental NMR techniques. These techniques have been developed over half a century of intensive research, and grown so advanced that a recent book on the subject is entitled "Spin Choreography" [21]. It is noteworthy that, due to the scope of its applications, NMR is now more often studied in chemistry and even biochemistry than it is in physics and engineering, where it was initially developed. This has had the effect that a large portion of these techniques have been discovered empirically and put into the form of intuitive graphical or algebraic rules, rather than developed mathematically from well-defined principles. Thus the interest which NMR computing is attracting from the quantum information processing side likewise has the potential to benefit the field of NMR spectroscopy, particularly through the application of algorithmic, information theoretic and algebraic techniques.

Finally, NMR has the potential to contribute in significant ways to the development of its own mathematics, in the same ways that computers have contributed to the development of recursive function theory, number theory, combinatorics and many other areas of mathematics. By performing experiments which can be interpreted as computations in homomorphic images on the algebras that are naturally associated with NMR spectroscopy, it may be possible to obtain insights into, or even "proofs" of, algebraic properties that would other-

wise be inaccessible. To give some idea of its potential computational power, we point out that the spin dynamics of a crystal of calcium fluoride one millimeter on a side, which can be highly polarized, superbly controlled and measured in microscopic detail by NMR techniques [53, 57], is described by an exponential map in an algebra on about $4^{10^{11}}$ physically distinct dimensions.

This paper will survey our recent research on quantum information processing by liquid-state NMR spectroscopy, including some new experiments which serve to clarify the underlying principles. We begin with a geometric interpretation of the quantum mechanical states and operators of an ensemble of identical spin 1/2 particles, both pure and mixed, which provides considerable insight into NMR. The corresponding geometric algebra is then extended to the *product operator formalism*, which is widely used in analyzing NMR experiments, and which constitutes a facile framework within which to study quantum information processing more generally [48]. We proceed to use this formalism to give an overview of the basic ideas behind ensemble quantum computing by liquid-state NMR spectroscopy, with emphasis on “pseudo-pure” state preparation and scaling. Next, we consider one way in which quantum correlations can appear to be present even in weakly polarized spin ensembles, and illustrate this with the results of NMR experiments which constitute a macroscopic analogue of Hardy’s paradox [26]. Finally, the utility of NMR and its associated product operator formalism as a means of studying decoherence will be demonstrated by an analysis of our recent experiments with a three-bit quantum error correcting code [15].⁴

2 The geometry of spin states and operators

NMR spectroscopy is based on the fact that the nuclei in many kinds of atoms are endowed with an intrinsic angular momentum, the properties of which are determined by an integer or half-integer quantum number $S \geq 0$, called the nuclear *spin*. For the purposes of quantum information processing by NMR, it will suffice to restrict ourselves to spin $S = 1/2$. In this case, measurement of the component of the angular momentum along a given axis in space always yields one of two possible values: $\pm\hbar/2$ (where \hbar is Planck’s constant h over 2π).

⁴ The reader is assumed throughout to be familiar with the basic notions of quantum information processing, as presented in e.g. Refs. [43, 44, 51, 56]. Excellent detailed expositions of NMR spectroscopy are also available, see e.g. Refs. [19, 21, 40, 47]. A more introductory account of our work on ensemble quantum computing by NMR spectroscopy, directed primarily towards physicists, may be found in Ref. [16].

According to the principles of quantum mechanics, the quantum state of the “spin” (nucleus) after such a measurement may be completely characterized by one of two orthonormal vectors in a two-dimensional Hilbert (complex vector) space \mathcal{H} , with Hermitian (sesquilinear) inner product $\langle \cdot | \cdot \rangle$. A rotation of this axis in physical space induces a transformation in \mathcal{H} by an element of the special unitary group $SU(2)$, which is the two-fold universal covering group of the three-dimensional Euclidean rotation group $SO(3)$, and the elements of \mathcal{H} are called *spinors* to emphasize this fact. The Lie algebra basis $(\mathbf{I}_x, \mathbf{I}_y, \mathbf{I}_z)$ of $SU(2)$ (or $SO(3)$) corresponding to infinitesimal rotations about three orthogonal axes in space satisfies the commutation relations

$$[\mathbf{I}_x, \mathbf{I}_y] = i\mathbf{I}_z, \quad [\mathbf{I}_z, \mathbf{I}_x] = i\mathbf{I}_y, \quad [\mathbf{I}_y, \mathbf{I}_z] = i\mathbf{I}_x, \quad (1)$$

and the eigenvalues $\pm 1/2$ of these three Hermitian (self-adjoint) operators correspond to the possible outcomes of measurements of the angular momentum (in units of \hbar) along the three axes.⁵

The Hilbert space representation of the kinematics of an isolated spin, however, is not sufficient to describe the joint state of the macroscopic collections of spins which are the subject of NMR spectroscopy. A *mixed state* (as opposed to the *pure state* of an isolated spin) is a random *ensemble* of spins not all in the same pure state. This “ensemble” could be a thought-construction which describes our state-of-knowledge of a single spin (as used in J. W. Gibbs’ formulation of statistical thermodynamics), or it could be a very large physical collection of spins, as in an NMR sample tube. In either case, a probability is assigned to every possible spinor, which can be interpreted as its frequency of occurrence in the ensemble (but see Ref. [30] for a Bayesian point-of-view). The Heisenberg uncertainty principle limits what can be known about the ensemble to the *ensemble-average expectation values* of the quantum mechanical observables. This information, in turn, can be encoded into a single operator on \mathcal{H} , called the *density operator*.

To define this operator mathematically, we first recall the canonical algebra isomorphism between the endomorphisms $\text{End}(\mathcal{H})$ and the tensor product $\mathcal{H} \otimes \mathcal{H}^*$ of \mathcal{H} with its dual space \mathcal{H}^* . Denoting the dual of a vector $|\psi\rangle$ under the Hermitian inner product of \mathcal{H} by $\langle\psi|$, the composition product in $\text{End}(\mathcal{H})$

⁵ Detailed explanations of these basic features of the quantum mechanics of spin may be found in modern textbooks. We would particularly recommend Sakurai [45], for an introduction to the underlying physics, or the monograph by Biedenharn and Louck [5], for a complete mathematical development.

corresponds to a product on $\mathcal{H} \otimes \mathcal{H}^*$ which is given on the factorizable tensors by

$$(|\varphi\rangle \otimes \langle \varphi'|)(|\vartheta\rangle \otimes \langle \vartheta'|) = \langle \varphi' | \vartheta \rangle (|\varphi\rangle \otimes \langle \vartheta'|), \quad (2)$$

and extended to all tensors by linearity. Following common practice, we shall usually drop the tensor product sign “ \otimes ” and write this *dyadic product* as $|\varphi\rangle\langle\vartheta|$. The restriction of this product to the diagonal, $|\psi\rangle\langle\psi|$, linearly spans the (real) subspace of all Hermitian operators in $\text{End}(\mathcal{H})$, and the action of $\text{SU}(2)$ on these products is its usual action on such operators,

$$|\psi\rangle\langle\psi| \mapsto \mathbf{U} |\psi\rangle\langle\psi| \tilde{\mathbf{U}}, \quad (3)$$

where $\tilde{\mathbf{U}} \equiv \mathbf{U}^\sim$ denotes the Hermitian conjugate (adjoint) of $\mathbf{U} \in \text{SU}(2)$.

Restricting ourselves to an ensemble involving a finite set of states $\{|\psi_k\rangle\}$ for ease of presentation, the density operator may now be defined as [7]

$$\boldsymbol{\rho} \equiv \overline{|\psi\rangle\langle\psi|} \equiv \sum_k p_k |\psi_k\rangle\langle\psi_k|, \quad (4)$$

where the $p_k \geq 0$ are the probabilities of the various states in the ensemble ($\sum_k p_k = 1$). Because $\langle\varphi|\boldsymbol{\rho}|\varphi\rangle = \sum_k p_k |\langle\varphi|\psi_k\rangle|^2 \geq 0$ for any spinor $|\varphi\rangle$, the density operator is necessarily positive semi-definite. Letting “tr” be the contraction operation on $\mathcal{H} \otimes \mathcal{H}^*$ (or trace on $\text{End}(\mathcal{H})$), letting $\mathbf{A} \in \text{End}(\mathcal{H})$ be any Hermitian operator, and using the invariance of the trace under cyclic permutations, we find that

$$\text{tr}(\mathbf{A}\boldsymbol{\rho}) = \sum_k p_k \text{tr}(\mathbf{A}|\psi_k\rangle\langle\psi_k|) = \sum_k p_k \langle\psi_k|\mathbf{A}|\psi_k\rangle. \quad (5)$$

This proves our claim that all ensemble-average expectation values can be obtained from $\boldsymbol{\rho}$. Note in particular that $\text{tr}(\boldsymbol{\rho}) = 1$.

Before showing how this applies to NMR spectroscopy, we wish to introduce an important geometric interpretation of the spin 1/2 density operator, and indeed of the entire operator algebra. As operators, the angular momentum components transform under $\text{SU}(2)$ by conjugation, i.e. $\mathbf{I}_w \mapsto \mathbf{U}\mathbf{I}_w\tilde{\mathbf{U}}$ ($w \in \{x, y, z\}$). Thus \mathbf{U} and $-\mathbf{U}$ induce the same transformation, so that conjugation constitutes a transitive group action of $\text{SO}(3)$ on the real linear space $\langle\mathbf{I}_x, \mathbf{I}_y, \mathbf{I}_z\rangle$. It follows that this space is naturally regarded as a three-dimensional Euclidean vector space. Note further that $\langle\mathbf{1}, \mathbf{I}_x, \mathbf{I}_y, \mathbf{I}_z\rangle$ equals the four-dimensional space of Hermitian operators on \mathcal{H} , where $\mathbf{1}$ is the identity on \mathcal{H} which we will henceforth identify with the scalar identity 1. This shows that any density operator can be uniquely expanded as the sum of a *scalar* and a *vector*:

$$\boldsymbol{\rho} = \frac{1}{2} \text{tr}(\boldsymbol{\rho}) + \text{tr}(\mathbf{I}_x \boldsymbol{\rho}) 2\mathbf{I}_x + \text{tr}(\mathbf{I}_y \boldsymbol{\rho}) 2\mathbf{I}_y + \text{tr}(\mathbf{I}_z \boldsymbol{\rho}) 2\mathbf{I}_z \equiv \frac{1}{2}(1 + \mathbf{P}) \quad (6)$$

We call \mathbf{P} the *polarization vector*, since its length $P \equiv \|\mathbf{P}\| \leq 1$ (the polarization) is a measure of the overall degree of alignment of the spins in the ensemble along \mathbf{P} . The positive semi-definiteness of ρ implies $P \leq 1$, and if $P = 1$, the density operator describes a (ensemble of spins in the same) pure state up to an overall phase factor. In this latter case the density operator can be written as $\rho = |\psi\rangle\langle\psi|$ for some spinor $|\psi\rangle$, and hence is *idempotent* (equal to its square). This vectorial interpretation of two-state quantum systems became widely known through the work of Feynman, Vernon and Helwarth [20], although it is inherent in the phenomenological equations for NMR first proposed by F. Bloch [6] (see below).

To extend this geometric interpretation to the entire algebra generated by $\langle \mathbf{1}, \mathbf{I}_x, \mathbf{I}_y, \mathbf{I}_z \rangle$, we regard the composition product of angular momentum operators as an associative bilinear product of vectors. We shall call this the *geometric vector product*. Since the eigenvalues of the ($S = 1/2$) angular momentum operators are $\pm 1/2$, the eigenvalues of their squares are both $1/4$, from which it follows that $(2\mathbf{I}_x)^2 = (2\mathbf{I}_y)^2 = (2\mathbf{I}_z)^2 = 1$. In accord with the isotropy of space, moreover,

$$(\mathbf{U}\mathbf{I}_w\tilde{\mathbf{U}})^2 = \mathbf{U}(\mathbf{I}_w)^2\tilde{\mathbf{U}} = 1/4 \quad (7)$$

for all $\mathbf{U} \in \text{SU}(2)$ and $w \in \{x, y, z\}$, which together with the bilinearity of the product implies that the square of *any* vector is equal (relative to the orthonormal basis $(2\mathbf{I}_x, 2\mathbf{I}_y, 2\mathbf{I}_z)$) to its length squared. Via the law of cosines, we can now show that the *symmetric part* of the geometric product of any two vectors is their usual Euclidean inner product:

$$\begin{aligned} \mathbf{A} \cdot \mathbf{B} &= \frac{1}{2} (\|\mathbf{A}\|^2 + \|\mathbf{B}\|^2 - \|\mathbf{A} - \mathbf{B}\|^2) \\ &= \frac{1}{2} (\mathbf{A}^2 + \mathbf{B}^2 - (\mathbf{A} - \mathbf{B})^2) = \frac{1}{2} (\mathbf{A}\mathbf{B} + \mathbf{B}\mathbf{A}) \end{aligned} \quad (8)$$

The commutation relations in Eq. (1), on the other hand, show that the *antisymmetric part* is equal (up to a factor of $-\imath$) to the usual vector cross product:

$$\mathbf{A} \times \mathbf{B} = -\frac{\imath}{2} [\mathbf{A}, \mathbf{B}] = -\frac{\imath}{2} (\mathbf{A}\mathbf{B} - \mathbf{B}\mathbf{A}) \equiv -\imath(\mathbf{A} \wedge \mathbf{B}) \quad (9)$$

We call the antisymmetric part $\mathbf{A} \wedge \mathbf{B} = \imath(\mathbf{A} \times \mathbf{B})$ the *outer product* of \mathbf{A} and \mathbf{B} , and note that it is geometrically distinct from vectors because inversion in the origin does not change it. Such things have been called “axial vectors”, although we prefer the older and more descriptive term *bivector*. On writing the geometric product as the sum of its symmetric and antisymmetric parts, $\mathbf{A}\mathbf{B} = \mathbf{A} \cdot \mathbf{B} + \mathbf{A} \wedge \mathbf{B}$, we see that perpendicular pairs of vectors anticommute. It follows that the three basis bivectors $\imath 2\mathbf{I}_x$, $\imath 2\mathbf{I}_y$ and $\imath 2\mathbf{I}_z$ also anticommute.

These square to -1 rather than 1 , however, and thus can be identified with the usual *quaternion* units [1]. Finally, the *unit pseudo-scalar* $8\mathbf{I}_x\mathbf{I}_y\mathbf{I}_z$ likewise squares to -1 , which together with the fact that it commutes with the basis vectors and hence everything in the algebra enables it to be identified with the unit imaginary i itself [25].

This algebra is often called the *Clifford algebra* of a three-dimensional Euclidean vector space, although we shall use the term *geometric algebra* here (which W. K. Clifford himself used). Such an algebra is canonically associated with any metric vector space, and provides a natural algebraic encoding of the geometric properties of that space. The fact that the three-dimensional Euclidean version can be defined starting from the well-known properties of the spin $1/2$ angular momentum operators indicates that a large part of quantum mechanics is really just an unfamiliar (but extremely elegant and facile [27, 29]) means of doing Euclidean geometry. Geometric algebra has more recently been extensively advocated and used to demystify quantum physics by a number of groups [4, 17, 28, 38]. Of particular interest are recent proposals to use the geometric algebra of a direct sum of copies of Minkowski space-time to obtain a relativistic multiparticle theory, from which all the nonrelativistic theory used in this paper falls out naturally as a quotient subalgebra [18].

We are now ready to describe the simplest possible NMR experiment. The time-independent Schrodinger equation is

$$i\hbar|\dot{\psi}\rangle = \mathbf{H}|\psi\rangle, \quad (10)$$

where the Hamiltonian \mathbf{H} is the generator of motion and the “dot” denotes the time derivative. This implies that the density operator evolves according to the *Liouville-von Neumann equation*:

$$\begin{aligned} i\hbar\dot{\rho} &= i\hbar\sum_k p_k \left(|\dot{\psi}_k\rangle\langle\psi_k| + |\psi_k\rangle\langle\dot{\psi}_k| \right) \\ &= \sum_k p_k \left(\mathbf{H}|\psi_k\rangle\langle\psi_k| - |\psi_k\rangle\langle\psi_k|\mathbf{H} \right) = [\mathbf{H}, \rho] \end{aligned} \quad (11)$$

The dominant Hamiltonian in NMR is the Zeeman interaction of the magnetic dipoles of the spins (which is parallel to their angular momentum vectors) with a constant applied magnetic field \mathbf{B}_0 . This *Zeeman Hamiltonian* is given by $\mathbf{H}_Z = -\frac{1}{2}\gamma\hbar\mathbf{B}_0$, where γ is a proportionality constant called the *gyromagnetic ratio*, which together with the above gives the *Bloch equation* [6]:

$$\dot{\mathbf{P}} = \dot{\rho} = -i\frac{1}{2}\gamma[\rho, \mathbf{B}_0] = \gamma\mathbf{P} \times \mathbf{B}_0 \quad (12)$$

The solution to this equation is $\rho(t) = \mathbf{U}\rho(0)\tilde{\mathbf{U}}$ with $\mathbf{U} = \exp(-it\mathbf{H}_Z)$, which is a time-dependent rotation of the polarization vector about the magnetic field

with a constant angular velocity $\omega_0 \equiv \gamma \hbar \|\mathbf{B}_0\|$. This “classical” picture is an example of Ehrenfest’s theorem, and is analogous to the precession of a gyroscope in a gravitational field.

Throughout this paper we adopt the universal convention that the magnetic field is along the z-axis: $\mathbf{B}_0 = B_0 2\mathbf{I}_z$. The component of the net precessing magnetic moment of the spins in the transverse xy-plane generates a complex-valued radio-frequency electrical signal proportional to $\text{tr}((\mathbf{I}_x + i\mathbf{I}_y)\rho(t)) = 2\mathbf{I}_x \cdot \mathbf{P}(t) + i2\mathbf{I}_y \cdot \mathbf{P}(t)$, whose Fourier transform is an NMR spectrum containing a peak at the precession frequency of each distinct kind of spin present in the sample. This has the important consequence that in NMR we measure the *expectation values* of the observables directly, which is due in turn to the fact that we are measuring the sum of the responses of the spins over the ensemble. These measurements yield negligible information on the quantum state of the individual spins in the ensemble and hence are nonperturbing, in that they do not appreciably change the state of the ensemble as a whole. Such *weak measurements* contrast starkly with the strong measurements usually considered in quantum mechanics, where determining the component of a spin along an axis yields one of two possible values and “collapses” it into the corresponding basis state, so that only one classical bit of information can be obtained [43, 45]. A discussion of the computational implications of weak measurements may be found in Ref. [14].

The natural (minimum energy) orientation of the spins’ dipoles in a magnetic field is parallel to the field, and thus to obtain a precessing magnetic dipole it is necessary to rotate the polarization vector \mathbf{P} away from the field axis $2\mathbf{I}_z$. This is done by applying an additional, rotating magnetic field \mathbf{B}_1 of magnitude B_1 in the xy-plane perpendicular to the static field \mathbf{B}_0 , which gives the time-dependent Hamiltonian

$$\mathbf{H} = \mathbf{H}_Z + \mathbf{H}_{\text{RF}} = -\gamma \hbar (B_0 \mathbf{I}_z + B_1 (\cos(\omega t) \mathbf{I}_x + \sin(\omega t) \mathbf{I}_y)) . \quad (13)$$

The effect of such a rotating field is most easily determined by transforming everything into a frame which rotates along with it, in which the Hamiltonian becomes time-independent:

$$\rho' = e^{-i\omega t \mathbf{I}_z} \rho e^{i\omega t \mathbf{I}_z} , \quad \mathbf{H}' = e^{-i\omega t \mathbf{I}_z} \mathbf{H} e^{i\omega t \mathbf{I}_z} = \mathbf{H}_Z + \gamma \hbar B_1 \mathbf{I}_x \quad (14)$$

Then the Bloch equation itself is transformed as follows:

$$\begin{aligned} \dot{\mathbf{P}}' &= -i\omega \mathbf{I}_z \mathbf{P}' + e^{-i\omega t \mathbf{I}_z} \dot{\mathbf{P}} e^{i\omega t \mathbf{I}_z} + \mathbf{P}' i\omega \mathbf{I}_z \\ &= \mathbf{P}' \times (\mathbf{H}' - \omega \mathbf{I}_z) \end{aligned} \quad (15)$$

Thus if ω equals the natural precession frequency of the spins $\omega_0 = \gamma\hbar B_0$, the Zeeman Hamiltonian $\mathbf{H}'_Z = \mathbf{H}_Z = \omega_0 \mathbf{I}_z$ cancels out. In this frame, the spins turn about a (rotating) axis perpendicular to \mathbf{B}'_1 at a rate $\omega_1 = \gamma\hbar B_1$, so that if the polarization vector starts out along \mathbf{z} , it is in the xy -plane where it produces the maximum signal after a time $t = \pi/(2\omega_1)$. Henceforth, all our coordinate frames will be rotating at the transmitter frequency unless otherwise mentioned.

3 The product operator formalism

Thus far we have restricted our presentation to ensembles consisting of indistinguishable nuclear spins. The power of NMR spectroscopy as a means of chemical analysis, however, depends on the fact that the different nuclei in a molecule generally have distinct electronic environments, which affect the applied magnetic field at each nucleus. As a result, they precess at slightly different frequencies and give rise to resolvable “peaks” in the resulting spectrum. This is also one of the reasons why NMR provides a facile approach to quantum information processing, since it permits each *chemical* equivalence class of spins in the ensemble to be treated as a separate “qubit”. In this section we will describe an extension of the density operator to multispin systems, using a basis which is a direct generalization of the “scalar + vector” basis given above for a single spin. We then illustrate this so-called *product operator formalism* [8, 19, 48, 50, 54] by describing how quantum information processing can be done on an ensemble of multispin molecules, using the internal Hamiltonian of liquid-state NMR. For the sake of simplicity we shall assume throughout that the ensemble is in a pure state, i.e. that the joint state of the spins in every molecule is identical. The next section is devoted to the complications involved in extending this approach to the highly mixed states which are available in practice.

As usual in quantum information processing [51, 56], we choose a *computational basis* ($|0\rangle, |1\rangle$) for the Hilbert space \mathcal{H} of each spin that corresponds to the eigenvectors of its \mathbf{I}_z operator, i.e. to alignment of the spin with (up) and against (down) a magnetic field \mathbf{B}_0 along the z axis. Relative to this basis, a superposition $c_0|0\rangle + c_1|1\rangle$ ($c_0, c_1 \neq 0$ complex with $|c_0|^2 + |c_1|^2 = 1$) is any state with transverse (xy) components. The Hilbert space needed to describe the kinematics of a system consisting of N distinguishable spins (*not* an ensemble) is the N -fold tensor product of their constituent Hilbert spaces [43, 45]. The induced basis in this (2^N) -dimensional space is

$$|\kappa^1\rangle \otimes |\kappa^2\rangle \otimes \cdots \otimes |\kappa^N\rangle \equiv |\kappa^1\kappa^2 \dots \kappa^N\rangle \equiv |k\rangle, \quad (16)$$

where $\kappa^n \in \{0, 1\}$ ($n = 1, \dots, N$) is the binary expansion of the integer $k \in \{0, \dots, 2^N - 1\}$. Because of the canonical isomorphism

$$\text{End}(\mathcal{H}) \otimes \text{End}(\mathcal{H}) \approx \text{End}(\mathcal{H} \otimes \mathcal{H}) \quad (17)$$

together with our previous isomorphism $\text{End}(\mathcal{H}) \approx \mathcal{H} \otimes \mathcal{H}^*$, this implies that the density operators for an ensemble of N -spin molecules are all contained in the N -fold tensor product space

$$(\mathcal{H} \otimes \dots \otimes \mathcal{H}) \otimes (\mathcal{H}^* \otimes \dots \otimes \mathcal{H}^*) \approx (\mathcal{H} \otimes \mathcal{H}^*) \otimes \dots \otimes (\mathcal{H} \otimes \mathcal{H}^*). \quad (18)$$

It follows that a basis for the algebra of N -spin operators is

$$\begin{aligned} |k\rangle\langle\ell| &= |\kappa^1 \kappa^2 \dots \kappa^N\rangle\langle\lambda^1 \lambda^2 \dots \lambda^N| \\ &= (|\kappa^1\rangle\langle\lambda^1|) \otimes (|\kappa^2\rangle\langle\lambda^2|) \otimes \dots \otimes (|\kappa^N\rangle\langle\lambda^N|), \end{aligned} \quad (19)$$

where $\kappa^n, \lambda^n \in \{0, 1\}$ ($n = 1, \dots, N$) are binary expansions of the integers $k, \ell \in \{0, \dots, 2^N - 1\}$. This basis, however, does not consist of Hermitian operators, and although the dyadic products $|\psi\rangle\langle\psi|$ ($|\psi\rangle \in \mathcal{H} \otimes \dots \otimes \mathcal{H}$) do span the real subspace of all Hermitian operators, the restriction of the basis in Eq. (19) to the diagonal does not.

An algebra basis which has the advantage of also being a linear basis for the subspace of Hermitian operators is known as the *product operator basis*. It is induced by the one-spin basis $(\mathbf{1}, \mathbf{I}_x, \mathbf{I}_y, \mathbf{I}_z)$, and consists simply of the tensor products of the angular momentum operators of the individual spins. In the case of two spins, this basis has sixteen elements:

$$\begin{aligned} &\mathbf{1} \otimes \mathbf{1} \quad \mathbf{1} \otimes \mathbf{I}_x \quad \mathbf{1} \otimes \mathbf{I}_y \quad \mathbf{1} \otimes \mathbf{I}_z \\ &\mathbf{I}_x \otimes \mathbf{1} \quad \mathbf{I}_x \otimes \mathbf{I}_x \quad \mathbf{I}_x \otimes \mathbf{I}_y \quad \mathbf{I}_x \otimes \mathbf{I}_z \\ &\mathbf{I}_y \otimes \mathbf{1} \quad \mathbf{I}_y \otimes \mathbf{I}_x \quad \mathbf{I}_y \otimes \mathbf{I}_y \quad \mathbf{I}_y \otimes \mathbf{I}_z \\ &\mathbf{I}_z \otimes \mathbf{1} \quad \mathbf{I}_z \otimes \mathbf{I}_x \quad \mathbf{I}_z \otimes \mathbf{I}_y \quad \mathbf{I}_z \otimes \mathbf{I}_z \end{aligned} \quad (20)$$

As before, a notation which eliminates the need for repetitive “ \otimes ” symbols is preferred. This is obtained by using superscripts for the spin indices in the operators

$$\mathbf{I}_w^n \equiv \mathbf{1} \otimes \dots \otimes \mathbf{1} \otimes \mathbf{I}_w \otimes \mathbf{1} \otimes \dots \otimes \mathbf{1} \quad (21)$$

(\mathbf{I}_w in the n -th place, $n = 1, \dots, N$, $w \in \{x, y, z\}$), and noting that by the *mixed product formula* between the operator composition and tensor products:

$$\mathbf{I}_u^m \mathbf{I}_v^n = \mathbf{1} \otimes \dots \otimes \mathbf{I}_u \otimes \mathbf{1} \otimes \dots \otimes \mathbf{1} \otimes \mathbf{I}_v \otimes \dots \otimes \mathbf{1} = \mathbf{I}_v^n \mathbf{I}_u^m \quad (22)$$

(\mathbf{I}_u in the m -th place, \mathbf{I}_v in the n -th, $m, n = 1, \dots, N$ with $m < n$, and $u, v \in \{x, y, z\}$). In the following, we will again identify the identity operator $\mathbf{1} \otimes \dots \otimes \mathbf{1}$ with the scalar identity 1. We will also be using the operator norm $\|\mathbf{I}_w^n\|^2 \equiv \langle (\mathbf{I}_w^n)^2 \rangle = (\mathbf{I}_w^n)^2 = 1/4$ obtained from the scalar part, rather than the more usual Frobenius norm $\|\mathbf{I}_w^n\|_F^2 = \text{tr}((\mathbf{I}_w^n)^2) = 2^{N-2}$ on $\text{End}(\mathcal{H})$, because the former is independent of N . The normalization of our basis to $\|\mathbf{I}_w^n\| = 1/2$ rather than 1 will be seen to have both advantages and disadvantages, but the convention is well-established in NMR.

Just as with an ensemble consisting of a single type of spin, a pure state may be characterized by the idempotence of its density operator: $\rho^2 = \rho$. The scalar part of the density operator is $\langle \rho \rangle = 2^{-N} \text{tr}(\rho) = 2^{-N}$, and if we write an arbitrary density operator $\rho \equiv |\psi\rangle\langle\psi|$ in diagonal form as

$$\rho = \mathbf{U} \left(\sum_{k=0}^{2^N-1} p_k |k\rangle\langle k| \right) \tilde{\mathbf{U}} \quad (23)$$

($0 \leq p_k \leq 1$, $\sum_k p_k = 1$) for some $\mathbf{U} \in \text{SU}(2^N)$, we see that the idempotence of ρ is equivalent to $\langle \rho^2 \rangle = 2^{-N}$, i.e. $p_\ell = 1$ for some $\ell \in \{0, \dots, 2^N - 1\}$. This shows that the density operator of a pure state is in fact a primitive idempotent. Without loss of generality we may take $\ell = 0$, so that $\rho = \mathbf{U} |00\dots 0\rangle\langle 00\dots 0| \tilde{\mathbf{U}}$. If we expand $|0\rangle\langle 0|$ in the product operator basis, we obtain $\mathbf{E}_+ \equiv \frac{1}{2}(1 + 2\mathbf{I}_z)$, and similarly for $|1\rangle\langle 1| = \mathbf{E}_- \equiv \frac{1}{2}(1 - 2\mathbf{I}_z)$. Thus we can also write the density operator of a pure state as

$$\rho = \mathbf{U} \left(\mathbf{E}_+^1 \mathbf{E}_+^2 \dots \mathbf{E}_+^N \right) \tilde{\mathbf{U}}, \quad (24)$$

where the superscript on the idempotent \mathbf{E}_+ is the spin index as before. More generally, the set of all density operators consists of the closed convex cone of positive semi-definite operators in the Hermitian subspace of $\text{End}(\mathcal{H} \otimes \dots \otimes \mathcal{H})$, and the density operators of pure states are the extreme rays of this cone.

We now consider the form of the Hamiltonian which is operative among the spins of an ensemble of molecules in the liquid state (with which we are exclusively concerned in this paper), again using the product operator formalism. First, there is the Zeeman Hamiltonian previously given for a single spin, i.e.

$$\mathbf{H}_Z \equiv -\omega_0^1 \mathbf{I}_z^1 - \dots - \omega_0^N \mathbf{I}_z^N \quad (25)$$

with $\omega_0^n = \hbar \gamma^n (1 - \sigma^n) B_0$, where γ^n the gyromagnetic ratio of the n -th spin and $0 \leq \sigma^n \leq 1$ is the *chemical shift* due to the (usually small) influence of the electronic environment of the spins on their precession frequencies. This

Hamiltonian is easily seen to be diagonal in the computational basis $|k\rangle$ ($k = 0, \dots, 2^N - 1$), with eigenvalues $(\pm\omega_0^1 \pm \dots \pm \omega_0^N)/2$.

Second, there is an exchange interaction known as the J or *scalar coupling*, which is proportional to the inner product of the spins' polarization vectors, namely

$$\mathbf{H}_J = \sum_{m,n} 2\pi J^{mn} (\mathbf{I}_x^m \mathbf{I}_x^n + \mathbf{I}_y^m \mathbf{I}_y^n + \mathbf{I}_z^m \mathbf{I}_z^n) , \quad (26)$$

where J^{mn} is the coupling strength in Hertz. This interaction is mediated by the electrons in the chemical bonds between atoms, and is usually negligible for atoms separated by more than three bonds. Standard perturbation theory [45] shows that the eigenvalues of the total Hamiltonian $\mathbf{H} = \mathbf{H}_Z + \mathbf{H}_J$ are given to first order by the diagonal elements of

$$\mathbf{H}' = \mathbf{H}_Z + \mathbf{H}'_J \equiv \mathbf{H}_Z + 2\pi \sum_{m,n} J^{mn} \mathbf{I}_z^m \mathbf{I}_z^n , \quad (27)$$

whereas the eigenvectors are given to first order by:

$$|\ell\rangle' = |\ell\rangle + 2\pi \sum_{m,n} J^{mn} \sum_{k \neq \ell} \frac{\langle k | \mathbf{I}_x^m \mathbf{I}_x^n + \mathbf{I}_y^m \mathbf{I}_y^n + \mathbf{I}_z^m \mathbf{I}_z^n | \ell \rangle}{\langle \ell | \mathbf{H}_Z | \ell \rangle - \langle k | \mathbf{H}_Z | k \rangle} |k\rangle \quad (28)$$

The numerator of each term in the summations is nonzero only if $\kappa^p = \lambda^p$ for $p \neq m, n$ and $\kappa^m = (1 - \lambda^n)$, in which case it is πJ^{mn} , while the denominators of the corresponding terms are $\omega_0^m - \omega_0^n$. It follows that the eigenvectors are negligibly perturbed so long as the frequency *differences* are much larger than the scalar couplings, i.e. $|\omega_0^m - \omega_0^n| \gg \pi |J^{mn}|$. We shall be making this *weak coupling* approximation throughout.

Another, potentially quite large term in the molecular spin Hamiltonian is a through-space interaction between the spins' magnetic dipoles. Because of the rapid motions of the molecules in a liquid, however, these interactions are averaged to zero much more quickly than they can have any net effect. The effective absence of this interaction nevertheless has the important consequence that the *spins in different molecules do not interact*, and hence cannot be correlated with one another.⁶ As a result, the density operator of the entire sample ρ (which describes an abstract Gibbs ensemble obtained by tracing over the spins' environment) can be factorized into a product of density operators for the individual molecules, i.e.

$$\rho = \rho^1 \cdots \rho^M = \rho^1 \otimes \cdots \otimes \rho^M , \quad (29)$$

⁶ More precisely, the spins do not interact to an excellent, but first-order, approximation; second-order effects do exist and are a source of spin-spin relaxation (aka decoherence).

where $\rho^m \equiv \mathbf{1} \otimes \dots \otimes \rho^m \otimes \dots \otimes \mathbf{1}$. In a pure liquid (or if we are looking at just one component of a solution), all the molecules are equivalent so that all these density operators are the same. It follows that we can work with the partial trace over all but any one of the molecules, which is called the *reduced* density operator $\rho \equiv \rho^1 = \dots = \rho^M$. Since this operates on a space of dimension 2^N where N is now the number of spins in a single molecule, rather than 2^{MN} where $M \sim 10^{20}$ is the number of molecules in the sample, this is a very considerable simplification. It also means that in liquid-state NMR we are working with a physical ensemble (the sample), rather than a purely abstract Gibbs ensemble.

Finally, there is the interaction of the spins with a transverse RF (radio-frequency) field, which we described in the last section. Whenever weak coupling is valid, we can apply this field in a single ‘‘pulse’’, tuned to the precession frequency of the k -th spin (say), which is short enough that we may neglect the evolution of the spins due to scalar coupling while it lasts. This effects a unitary transformation of the form

$$\begin{aligned} e^{-i\theta \mathbf{I}_x^n} &= 1 - i \left(\frac{\theta}{2}\right) 2\mathbf{I}_x^n - \frac{1}{2} \left(\frac{\theta}{2}\right)^2 + \frac{i}{6} \left(\frac{\theta}{2}\right)^3 2\mathbf{I}_x^n + \dots \\ &= \cos\left(\frac{\theta}{2}\right) - i \sin\left(\frac{\theta}{2}\right) 2\mathbf{I}_x^n, \end{aligned} \quad (30)$$

which corresponds to a right-hand rotation of the k -th spin by an angle θ about the x axis in the rotating frame. Using a pulse with a broad frequency range, it is also possible (in fact easier) to apply such a rotation to all the spins in parallel.

We will now indicate how RF pulses, in combination with the innate Hamiltonian of the spins, enable us to implement standard quantum logic gates in a manner similar to that considered by computer scientists studying universality in quantum computation [3]. The simplest such gate is the NOT operation on the e.g. first spin, which simply rotates it by π ; combining the above formula with the basic geometric algebra relations $\mathbf{I}_x \mathbf{I}_z = -\mathbf{I}_z \mathbf{I}_x$ and $(2\mathbf{I}_x)^2 = 1$, we obtain

$$\begin{aligned} e^{-i\pi \mathbf{I}_x^1} \mathbf{E}_+^1 e^{i\pi \mathbf{I}_x^1} &= (-2i\mathbf{I}_x^1) \mathbf{E}_+^1 (2i\mathbf{I}_x^1) = \frac{1}{2}(1 + 8\mathbf{I}_x^1 \mathbf{I}_z^1 \mathbf{I}_x^1) \\ &= \frac{1}{2}(1 - 8\mathbf{I}_x^1 \mathbf{I}_x^1 \mathbf{I}_z^1) = \frac{1}{2}(1 - 2\mathbf{I}_z^1) = \mathbf{E}_-^1 \end{aligned} \quad (31)$$

The c-NOT (controlled-NOT) gate, on the other hand, is a π rotation of e.g. the first spin *conditional* on the polarization of a second. Using the relation $\mathbf{E}_\pm^2 \mathbf{E}_\mp^2 = 0$, we can easily show that

$$(-2i\mathbf{I}_x^1 \mathbf{E}_-^2 + \mathbf{E}_+^2)(\mathbf{E}_\epsilon^1 \mathbf{E}_\pm^2)(2i\mathbf{I}_x^1 \mathbf{E}_-^2 + \mathbf{E}_+^2) = \mathbf{E}_{\pm\epsilon}^1 \mathbf{E}_\pm^2 \quad (32)$$

($\epsilon \in \{\pm\}$). The phase factor i multiplying \mathbf{I}_x^1 complicates the action of the c-NOT on a superposition, but can be eliminated by a phase shift conditional on

the second spin. Using $\mathbf{E}_-^2 + \mathbf{E}_+^2 = 1$, this phase-corrected c-NOT gate is given by $\mathbf{S}^{1|2} \equiv$

$$\begin{aligned} 2\mathbf{I}_x^1 \mathbf{E}_-^2 + \mathbf{E}_+^2 &= (-i\mathbf{E}_-^2 + \mathbf{E}_+^2)(2i\mathbf{I}_x^1 \mathbf{E}_-^2 + \mathbf{E}_+^2) \\ &= \left(1 + (e^{-i\frac{\pi}{2}} - 1)\mathbf{E}_-^2\right) \left(1 + (e^{i\pi\mathbf{I}_x^1} - 1)\mathbf{E}_-^2\right) \\ &= e^{-i\frac{\pi}{2}} \mathbf{E}_-^2 e^{i\pi\mathbf{I}_x^1} \mathbf{E}_-^2 = e^{-i\frac{\pi}{2}(1-2\mathbf{I}_x^1)} \mathbf{E}_-^2, \end{aligned} \quad (33)$$

and hence the idempotents \mathbf{E}_\pm^n also give us an algebraic description of the c-NOT gate, in addition to the density operators of pure states. It is well-known that single spin rotations, together with the c-NOT, are sufficient to implement any quantum logic gate [3].

The c-NOT can be implemented in NMR by combining single spin rotations with the conditional rotations induced by (weak) scalar coupling $2\pi J^{12} \mathbf{I}_z^1 \mathbf{I}_z^2$ [16, 22, 31]. Recalling that in the discrete SO(3) subgroup of rotations by $\pi/2$,

$$e^{-i\frac{\pi}{2}\mathbf{I}_y^1} e^{i\frac{\pi}{2}\mathbf{I}_z^1} = e^{i\frac{\pi}{2}\mathbf{I}_z^1} e^{i\frac{\pi}{2}\mathbf{I}_x^1}, \quad (34)$$

we can expand the above propagator as follows:

$$\begin{aligned} \mathbf{S}^{1|2} &= e^{-i\frac{\pi}{2}(1-2\mathbf{I}_x^1)} \mathbf{E}_-^2 \\ &= e^{-i\frac{\pi}{2}\mathbf{I}_y^1} e^{-i\pi\mathbf{E}_-^1} \mathbf{E}_-^2 e^{i\frac{\pi}{2}\mathbf{I}_y^1} \\ &= \sqrt{-i} e^{-i\frac{\pi}{2}\mathbf{I}_y^1} e^{i\frac{\pi}{2}(\mathbf{I}_z^1 + \mathbf{I}_z^2)} e^{-i\pi\mathbf{I}_z^1 \mathbf{I}_z^2} e^{i\frac{\pi}{2}\mathbf{I}_y^1} \\ &= \sqrt{-i} e^{i\frac{\pi}{2}(\mathbf{I}_z^1 + \mathbf{I}_z^2)} e^{i\frac{\pi}{2}\mathbf{I}_x^1} e^{-i\pi\mathbf{I}_z^1 \mathbf{I}_z^2} e^{i\frac{\pi}{2}\mathbf{I}_y^1} \end{aligned} \quad (35)$$

Since the overall phase of the transformation has no effect on the density operator, it follows that the c-NOT gate $\mathbf{S}^{1|2}$ can be implemented by an NMR *pulse sequence*, wherein each pulse and delay corresponds to the indicated “effective” Hamiltonian in temporal order:

$$\begin{aligned} &[-\frac{\pi}{2}\mathbf{I}_y^1] \rightarrow [\pi\mathbf{I}_z^1 \mathbf{I}_z^2] \rightarrow [-\frac{\pi}{2}\mathbf{I}_x^1] \rightarrow [-\frac{\pi}{2}(\mathbf{I}_z^1 + \mathbf{I}_z^2)] \\ &\Leftrightarrow \exp\left(\frac{\pi}{2}(\mathbf{I}_z^1 + \mathbf{I}_z^2)\right) \exp\left(\frac{\pi}{2}\mathbf{I}_x^1\right) \exp(-\pi\mathbf{I}_z^1 \mathbf{I}_z^2) \exp\left(\frac{\pi}{2}\mathbf{I}_y^1\right) \end{aligned} \quad (36)$$

In practice, the effective Hamiltonian $[\pi\mathbf{I}_z^1 \mathbf{I}_z^2]$ is obtained by applying a π -pulse to both spins in the middle and at the end of a $1/(2J^{12})$ evolution period, to “refocus” their Zeeman evolution [16]. The $[-\frac{\pi}{2}\mathbf{I}_y^1]$ and $[-\frac{\pi}{2}\mathbf{I}_x^1]$ Hamiltonians are implemented by RF pulses as above, while the $[-\frac{\pi}{2}(\mathbf{I}_z^1 + \mathbf{I}_z^2)]$ transformation is most easily implemented by letting one spin evolve while applying a π -pulse to the other, then vice versa, and finally realigning the transmitter’s phase with the spins’.

The “readout” procedure needed to determine the result of an NMR computation differs somewhat that usually considered in quantum computing [51, 56]. The most important difference is of course the fact that in conventional NMR one can only make weak (nonperturbing) measurements of the observables, as previously described. As likewise described above, these observables are the x and y components \mathbf{I}_x^n and \mathbf{I}_y^n of the dipolar magnetization due to each spin in a rotating frame defined by the transmitter frequency. The products of the angular momentum components of different spins (e.g. $\mathbf{I}_x^1 \mathbf{I}_y^2$), however, do not produce a net magnetic dipole and hence cannot be detected directly. Thus we are limited to one-spin observables, as is usually assumed in quantum computation. The unobservable degrees of freedom may also be characterized in the basis $|k\rangle\langle\ell|$ as having a *coherence order* $|\langle k | \mathbf{I}_z | k \rangle - \langle \ell | \mathbf{I}_z | \ell \rangle| \neq 1$, where $\mathbf{I}_z \equiv \mathbf{I}_z^1 + \dots + \mathbf{I}_z^N$ is the total angular momentum along z [16, 19, 21, 40, 47].

According to the usual phase conventions of NMR, the Fourier transform of the x-magnetization of e.g. the first spin, \mathbf{I}_x^1 , yields an *absorptive* peak shape, while \mathbf{I}_y^1 produces a *dispersive* shape, both centered on its precession frequency ω_0^1 . If the first spin is coupled to e.g. the second, its signal is modulated by $\cos(\pi J^{12}t)$ yielding a spectrum containing two peaks separated by the coupling constant J^{12} [16]. An effective exception to the unobservability of the products are those of the form $\mathbf{I}_x^1 \mathbf{I}_z^2$ (or $\mathbf{I}_y^1 \mathbf{I}_z^2$), which (when $J^{12} \neq 0$) evolve under scalar coupling into one-spin terms. Using the facts that $4\mathbf{I}_z^1 \mathbf{I}_z^2$ and $4\mathbf{I}_x^1 \mathbf{I}_z^2$ anticommute while $(4\mathbf{I}_z^1 \mathbf{I}_z^2)^2 = 1$, we can show this as follows:

$$\begin{aligned} e^{-it\pi J^{12} 4\mathbf{I}_z^1 \mathbf{I}_z^2} (4\mathbf{I}_x^1 \mathbf{I}_z^2) &= e^{-it2\pi J^{12} \mathbf{I}_z^1 \mathbf{I}_z^2} (4\mathbf{I}_x^1 \mathbf{I}_z^2) e^{it2\pi J^{12} \mathbf{I}_z^1 \mathbf{I}_z^2} \\ &= (\cos(\pi J^{12}t) - i4\mathbf{I}_z^1 \mathbf{I}_z^2 \sin(\pi J^{12}t)) (4\mathbf{I}_x^1 \mathbf{I}_z^2) \quad (37) \\ &= \cos(\pi J^{12}t) 4\mathbf{I}_x^1 \mathbf{I}_z^2 + \sin(\pi J^{12}t) 2\mathbf{I}_y^1 \end{aligned}$$

Because the signal is now sinusoidally modulated by the coupling, for a single pair of coupled spins this results in a pair of *antiphase* peaks with opposite signs, as opposed to the *inphase* peaks described for \mathbf{I}_x^1 and \mathbf{I}_y^1 above. These antiphase peaks may likewise be absorptive ($\mathbf{I}_x^1 \mathbf{I}_z^2$) or dispersive ($\mathbf{I}_y^1 \mathbf{I}_z^2$), respectively. Figure 1 shows examples of all these possibilities for a pair of two coupled spins.

More generally, if the n -th spin is coupled to M others, its signal is split into 2^M peaks at frequencies of $(\omega_0^n/\pi \pm J^{m_1 n} \pm \dots \pm J^{m_M n})/2$, one for each combination of “up” and “down” states for the M spins to which it is coupled. If the transverse magnetization is due to a $\pi/2$ rotation of a spin polarized along z as before, then the heights of these peaks are proportional to the probability differences between pairs of states $|\kappa^{m_1} \dots \kappa^n \dots \kappa^{m_M}\rangle \leftrightarrow |\kappa^{m_1} \dots (1 - \kappa^n) \dots \kappa^{m_M}\rangle$

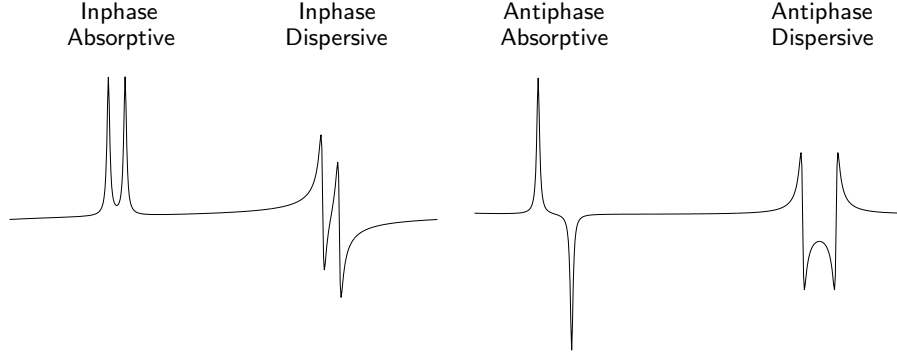


Fig. 1. Plots of NMR spectra for a weakly coupled two-spin molecule (amplitude versus frequency). The left-hand plot is for the spin state $\mathbf{I}_x^1 + \mathbf{I}_y^2$, which gives a pair of inphase absorptive peaks for spin 1 (left) and a pair of inphase dispersive peaks for spin 2 (right). The right-hand plot is for the spin state $\mathbf{I}_x^1 \mathbf{I}_z^2 + \mathbf{I}_z^1 \mathbf{I}_y^2$, which gives a pair of antiphase absorptive peaks for spin 1 (left) and a pair of antiphase dispersive peaks for spin 2 (right). By fitting the peak shapes in such spectra after various $\pi/2$ rotations of the individual spins, one obtains sufficient information to uniquely reconstruct the complete density operator.

separated by flips of that spin. To show this, we restrict ourselves to two spins for ease of presentation, and consider a general diagonal density operator of the form

$$\begin{aligned}
 \rho_{zz} &= p_0|00\rangle\langle 00| + p_1|01\rangle\langle 01| + p_2|10\rangle\langle 10| + p_3|11\rangle\langle 11| \\
 &= \frac{1}{4} + \frac{1}{2}(p_0 + p_1 - p_2 - p_3)\mathbf{I}_z^1 + \frac{1}{2}(p_0 - p_1 + p_2 - p_3)\mathbf{I}_z^2 \\
 &\quad + (p_0 - p_1 - p_2 + p_3)\mathbf{I}_z^1 \mathbf{I}_z^2,
 \end{aligned} \tag{38}$$

where p_k denotes the probability that a molecule is in the state $|k\rangle$. Rotating this to

$$\begin{aligned}
 \rho_{xz} &\equiv e^{-i\pi \mathbf{I}_y^1} \rho_{zz} e^{i\pi \mathbf{I}_y^1} \\
 &= \frac{1}{4} + \frac{1}{2}(p_0 + p_1 - p_2 - p_3)\mathbf{I}_x^1 + \frac{1}{2}(p_0 - p_1 + p_2 - p_3)\mathbf{I}_z^2 \\
 &\quad + (p_0 - p_1 - p_2 + p_3)\mathbf{I}_x^1 \mathbf{I}_z^2
 \end{aligned} \tag{39}$$

and computing the signal in the Zeeman frame yields

$$\begin{aligned}
& \text{tr} \left(e^{-it2\pi J^{12} \mathbf{I}_z^1 \mathbf{I}_z^2} \rho_{\text{xz}} e^{it2\pi J^{12} \mathbf{I}_z^1 \mathbf{I}_z^2} (\mathbf{I}_x^1 + i\mathbf{I}_y^1) \right) \\
&= \frac{1}{2} \left((p_0 + p_1 - p_2 - p_3) \cos(\pi J^{12} t) \right. \\
&\quad \left. + (p_0 - p_1 - p_2 + p_3) i \sin(\pi J^{12} t) \right) \\
&= \frac{1}{2} e^{i\pi J^{12} t} (p_0 - p_2) + \frac{1}{2} e^{-i\pi J^{12} t} (p_1 - p_3) ,
\end{aligned} \tag{40}$$

thus showing that the peaks at $\omega_0^1 \pm \pi J^{12}$ have amplitudes proportional to the probability differences as claimed.

In closing, we mention that although vector interpretations of single quantum inphase (\mathbf{I}_x^1) and antiphase ($\mathbf{I}_x^1 \mathbf{I}_z^2$) states are available (and widely used in NMR [21]), no satisfactory geometric interpretation of general product states is known. The development of an intuitive model for the geometry determined by the action of $\text{SU}(2^N)$ on the product operators thus stands as an open problem in the field. There are two reasons why the problem is nontrivial. The first is the well-known the existence of *correlated* states, whose density operators cannot be factorized; in the case of a pure state, these states are also called *entangled* [43]. We shall consider such states further in Section 5. The second, much less widely recognized reason is that there is but one imaginary unit for all the spins, so that in the tensor product of their geometric algebras the unit pseudo-scalars $8\mathbf{I}_x^n \mathbf{I}_y^n \mathbf{I}_z^n$ must be identified by taking an appropriate quotient [48]. This is a form of implicit correlation which is always present even in otherwise factorizable states. Further discussion of this issue may be found in Refs. [17, 18].

4 Pseudo-pure state preparation and scaling

Liquid state NMR must be done at temperatures far above the differences between the spin Hamiltonian's energy levels (eigenvalues). The ensemble's spin state thus represents a compromise between the constant force of the applied magnetic field and the forces of the random fields induced by the thermal motions of spins in other molecules. Thus pure states are not available, so that the underlying ensemble is not uniquely determined by its density operator. This would seem to make NMR useless as a means of performing deterministic computations, but in fact a class of mixed states has been found for which a state vector is (up to an overall phase) canonically associated with the density operator. This section is devoted to describing the properties and preparation of

such *pseudo-pure states*, with emphasis on the computationally important issue of how they scale with the number of spins N .

According to the principles of quantum statistical mechanics [7], the density operator ρ_{eq} for an ensemble of N -spin molecules at thermal equilibrium is given by the Boltzman operator determined by their common Hamiltonian, $\exp(-\mathbf{H}/k_{\text{B}}T)$, divided by the corresponding partition function $Z_{\text{eq}} = \text{tr}(\exp(-\mathbf{H}/k_{\text{B}}T))$ (where k_{B} is Boltzman’s constant). The Hamiltonian \mathbf{H} is well-approximated by its dominant Zeeman term $\mathbf{H}_{\text{Z}} = -\omega_0^1 \mathbf{I}_{\text{z}}^1 - \dots - \omega_0^N \mathbf{I}_{\text{z}}^N$. Given the gyromagnetic ratios of nuclear spins and the strongest available magnetic fields, we have $\|\mathbf{H}_{\text{Z}}\|/(k_{\text{B}}T) \sim 10^{-5}$ at the temperatures needed for liquid-state NMR, so that a linear approximation is quite accurate:

$$\rho_{\text{eq}} \approx \frac{1 - \mathbf{H}_{\text{Z}}/k_{\text{B}}T}{\text{tr}(1 - \mathbf{H}_{\text{Z}}/k_{\text{B}}T)} = \frac{1 - \mathbf{H}_{\text{Z}}/k_{\text{B}}T}{2^N} \quad (41)$$

In homonuclear (i.e. single spin isotope) systems, one can assume that $\omega_0^n \equiv \hbar B_0(1 - \sigma^n)\gamma^n \approx \hbar B_0\gamma$ is constant for all n . Since the amplitude of an NMR signal is also proportional to imprecisely known factors determined by the spectrometer setup, $\omega_0^n/(k_{\text{B}}T)$ is usually set to unity when analyzing a homonuclear experiment (or to the ratios of each γ^n with $\min_m(\gamma^m)$ otherwise). The partition function 2^{-N} is likewise constant for any given system, but because of our interest in scaling we shall always include it explicitly in this section.

It is important to observe that, because the angular momentum components observed by NMR have no scalar part (i.e. are traceless), the scalar part (identity component) of the density operator 2^{-N} does not contribute to the signal. It also does not evolve under unitary transformations, and hence NMR spectroscopists usually forget about it altogether — even though it comprises the vast majority of the norm of the density operator. In these terms, the equilibrium density operator of a two-spin system, and its matrix representation in the usual computational basis, is

$$\begin{aligned} \hat{\rho}_{\text{eq}} &= \frac{1}{4}(\mathbf{I}_{\text{z}}^1 + \mathbf{I}_{\text{z}}^2) = \frac{1}{4}(|00\rangle\langle 00| - |11\rangle\langle 11|) \\ \leftrightarrow \frac{1}{4} \mathbf{Diag}(1, 0, 0, -1) &\equiv \frac{1}{4} \begin{bmatrix} 1 & 0 & 0 & 0 \\ 0 & 0 & 0 & 0 \\ 0 & 0 & 0 & 0 \\ 0 & 0 & 0 & -1 \end{bmatrix}, \end{aligned} \quad (42)$$

where the “hat” on ρ_{eq} signifies its traceless part.

In contrast, the density operator of two spins in their pseudo-pure ground

(assuming $\gamma > 0$ as usual) state is

$$\begin{aligned}\hat{\rho}_{00} &\equiv \pm \frac{1}{6} (\mathbf{I}_z^1 + \mathbf{I}_z^2 + 2\mathbf{I}_z^1 \mathbf{I}_z^2) = \pm \frac{1}{3} (\mathbf{E}_+^1 \mathbf{E}_+^2 - \frac{1}{4}) \\ &= \pm \frac{1}{3} (|00\rangle\langle 00| - \frac{1}{4}) \leftrightarrow \pm \frac{1}{12} \mathbf{Diag}(3, -1, -1, -1).\end{aligned}\quad (43)$$

The overall sign depends on whether we have a population excess or deficit in the ground state; for consistency, we shall generally assume the former. Observe that a unitary transformation of the density operator induces a transformation of the corresponding state vector just as it does for true pure states, since

$$U \hat{\rho}_{00} \tilde{U} = \frac{1}{3} ((U|00\rangle)(U|00\rangle)^\sim - \frac{1}{4}). \quad (44)$$

Similarly, because the NMR observables $\mathbf{A} = \mathbf{I}_x^n, \mathbf{I}_y^n$ are traceless, the ensemble-average expectation value relative to a pseudo-pure density operator yields the ordinary expectation value versus the corresponding state vector:

$$\text{tr}(\mathbf{A} \hat{\rho}_{00}) = \frac{1}{3} (\text{tr}(\mathbf{A}|00\rangle\langle 00|) - \frac{1}{4} \text{tr}(\mathbf{A})) = \frac{1}{3} \langle 00 | \mathbf{A} | 00 \rangle \quad (45)$$

The general form of a pseudo-pure density operator is

$$\hat{\rho}_\psi = \frac{2^{N/2}}{2^N - 1} (|\psi\rangle\langle\psi| - 2^{-N}), \quad (46)$$

where $|\psi\rangle$ is a normalized N -spin state vector, and the prefactor has been chosen so as to keep the maximum eigenvalue $\|\hat{\rho}_\psi\|_2$ equal to that of the N -spin equilibrium density operator.

Even though we have defined them to have the same maximum eigenvalue, for $N > 1$ the remaining eigenvalues of $\hat{\rho}_{\text{eq}}$ and $\hat{\rho}_\psi$ differ, and hence there is no unitary transformation taking one to the other. There are nevertheless a number of nonunitary processes by which one can prepare pseudo-pure states. The most direct is to generate a spatially varying distribution of states across the sample, such that the ensemble average is pseudo-pure. This can be done by using a *field gradient* along the z-axis to create a position-dependent phase shift whose average is zero, thereby in effect setting the transverse (xy) components of the density operator to zero.⁷ For example, it is readily shown that the sequence

$$[\frac{\pi}{4}(\mathbf{I}_x^1 + \mathbf{I}_x^2)] \rightarrow [\pi \mathbf{I}_z^1 \mathbf{I}_z^2] \rightarrow [-\frac{\pi}{8}(\mathbf{I}_y^1 + \mathbf{I}_y^2)] \quad (47)$$

applied to the two-spin equilibrium state $\hat{\rho}_{\text{eq}}$ yields

$$2^{-\frac{5}{2}} \left(\sqrt{3} (\mathbf{E}_+^1 \mathbf{E}_+^2 - \frac{1}{4} - \mathbf{I}_x^1 \mathbf{I}_x^2) - \mathbf{I}_x^1 \mathbf{E}_-^2 - \mathbf{E}_-^1 \mathbf{I}_x^2 \right), \quad (48)$$

⁷ In the homonuclear case, the zero-quantum coherences are not rapidly dephased by a z-gradient, so a slightly more complicated procedure is necessary.

which is reduced by a z-gradient to $(3/32)^{\frac{1}{2}}(\mathbf{E}_+^1 \mathbf{E}_+^2 - 1/4)$. Further RF and gradient pulse sequences which convert the equilibrium state of two and three spin systems to pseudo-pure states may be found in Ref. [16].

An alternative proposed by E. Knill *et al.* [34] is to “time-average” the results of several separate experiments. In the simple case of a two spin system, the average of the three states

$$\begin{aligned}\hat{\rho}_{123} &\equiv \frac{1}{4}(\mathbf{I}_z^1 + \mathbf{I}_z^2) \leftrightarrow \frac{1}{4} \mathbf{Diag}(1, 0, 0, -1) \\ \hat{\rho}_{231} &\equiv \frac{1}{4}(\mathbf{I}_z^1 + 2\mathbf{I}_z^1 \mathbf{I}_z^2) \leftrightarrow \frac{1}{4} \mathbf{Diag}(1, 0, -1, 0) \\ \hat{\rho}_{312} &\equiv \frac{1}{4}(2\mathbf{I}_z^1 \mathbf{I}_z^2 + \mathbf{I}_z^2) \leftrightarrow \frac{1}{4} \mathbf{Diag}(1, -1, 0, 0)\end{aligned}\quad (49)$$

is the pseudo-pure state

$$\begin{aligned}\frac{1}{3}(\hat{\rho}_{123} + \hat{\rho}_{231} + \hat{\rho}_{312}) &= \frac{1}{12}(2\mathbf{I}_z^1 + 2\mathbf{I}_z^2 + 4\mathbf{I}_z^1 \mathbf{I}_z^2) \\ &\leftrightarrow \frac{1}{12} \mathbf{Diag}(3, -1, -1, -1).\end{aligned}\quad (50)$$

More generally, one can obtain the same results that one would get on a pseudo-pure state by averaging the results of the experiments over all $2^N - 1$ cyclic permutations of the nonground state populations of the equilibrium density operator. Although this naive approach is not efficient, Knill *et al.* have shown that one can average over smaller groups in time $O(N^3)$ with much the same effect.

A fundamentally different approach, first proposed by Stoll, Vega & Vaughan [52] and subsequently adapted to NMR computing by Gershenfeld & Chuang [22], involves working with subpopulations of molecules distinguished by the states of additional *ancilla* spins. Gershenfeld and Chuang [12] have given an example of a two-spin *conditional pseudo-pure state* (as we call it), which is obtained by row/column permutation of the diagonal equilibrium density matrix $\mathbf{Diag}(3, 1, 1, -1, 1, -1, -1, -3)/16$ of a three-spin system including one ancilla, namely

$$\begin{aligned}&\frac{1}{16} \mathbf{Diag}(3, -1, -1, -1, -3, 1, 1, 1) \\ \leftrightarrow &\frac{1}{16}(2\mathbf{I}_z^1(2\mathbf{I}_z^2 + 2\mathbf{I}_z^3 + 4\mathbf{I}_z^2 \mathbf{I}_z^3)) \\ = &\frac{1}{4}(\mathbf{E}_+^1 - \mathbf{E}_-^1)(\mathbf{E}_+^2 \mathbf{E}_+^3 - \frac{1}{4}).\end{aligned}\quad (51)$$

The last form makes it clear that in the subpopulation with the first spin “up”, which is labeled by \mathbf{E}_+^1 , and in the subpopulation with it “down”, which is labeled by \mathbf{E}_-^1 , spins 2 and 3 are in the pseudo-pure state $\mathbf{E}_+^2 \mathbf{E}_+^3 - 1/4$. Since the spectrum of spins 2 and 3 is antiphase with respect to the ancilla spin 1, one can select the subpopulations just by keeping only either positive or negative peaks. Although the situation is considerably more complicated with more spins,

Gershenfeld and Chuang have shown that conditional pure states can be obtained (with some loss of signal) using as few as $O(\log(N))$ ancillae.

An alternative to conditional pure states, which we call *relative pseudo-pure states*, can be obtained via the partial trace operation (in NMR, decoupling [19, 21, 40, 47]), rather than peak selection as above. For example, a two-spin relative pseudo-pure state is given by the partial trace over the ancilla spins 1 & 2 in

$$\begin{aligned} & \frac{1}{32} \mathbf{Diag}(4, 2, 2, 0, 2, 0, -2, 0, 0, -2, 0, 2, 0, -2, -2, -4) \\ \leftrightarrow & \frac{1}{16} (\mathbf{E}_+^1 \mathbf{E}_+^2 (\mathbf{E}_+^3 + \mathbf{E}_+^4) + \mathbf{E}_+^1 \mathbf{E}_-^2 (\mathbf{E}_+^3 \mathbf{E}_+^4 - \mathbf{E}_-^3 \mathbf{E}_+^4) \\ & + \mathbf{E}_-^1 \mathbf{E}_+^2 (\mathbf{E}_-^3 \mathbf{E}_-^4 - \mathbf{E}_+^3 \mathbf{E}_-^4) - \mathbf{E}_-^1 \mathbf{E}_-^2 (\mathbf{E}_-^3 + \mathbf{E}_-^4)) , \end{aligned} \quad (52)$$

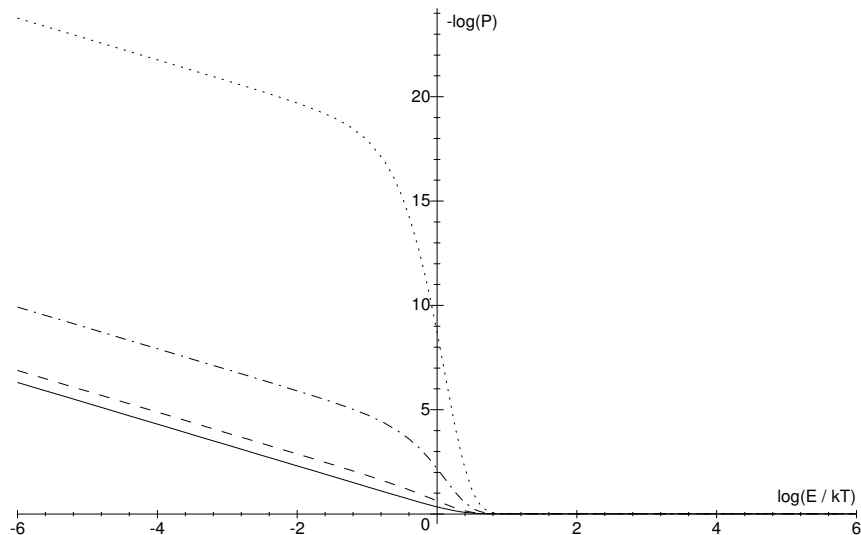
which is again a permutation of the diagonal elements of $\hat{\rho}_{\text{eq}}$. This can be seen by adding up the 4×4 blocks of the matrix, obtaining $\mathbf{Diag}(6, -2, -2, -2)/32$. Alternatively, since the partial trace in the product operator formalism corresponds to simply eliminating those terms depending on either spins 1 or 2 and multiplying the remaining terms by 4 [48], we need only add up the multipliers of $\mathbf{E}_+^1 \mathbf{E}_+^2, \dots, \mathbf{E}_-^1 \mathbf{E}_-^2$, which yields

$$\begin{aligned} & \frac{1}{16} ((1 + \mathbf{E}_+^3 - \mathbf{E}_-^3)(1 + \mathbf{E}_+^4 - \mathbf{E}_-^4) - 1) \\ = & \frac{1}{4} (\mathbf{E}_+^3 \mathbf{E}_+^4 - \frac{1}{4}) \leftrightarrow \frac{1}{32} \mathbf{Diag}(6, -2, -2, -2) . \end{aligned} \quad (53)$$

We now consider briefly how the SNR (signal-to-noise ratio) of these methods of creating pseudo-pure states scales with the number of spins N . It has been argued that since the equilibrium population of the ground state falls off exponentially with the number of spins, and all these methods are aimed in some fashion at isolating the signal from the ground state population, the SNR of all these methods must likewise decline exponentially with N [55]. Although this argument carries considerable weight, we shall see that the number and variety of the available methods renders the actual situation rather more complex. The standard to which the signal strength must be compared is that of a single spin in its equilibrium state, namely

$$\hat{\rho}_{\text{eq}} = \frac{1}{2} \mathbf{I}_z^1 = \frac{1}{4} (|0\rangle\langle 0| - |1\rangle\langle 1|) . \quad (54)$$

The maximum eigenvalue $\|\hat{\rho}_{\text{eq}}\|_2 = 1/4$ is what we will use as the standard signal strength for spins of like gyromagnetic ratio (as assumed throughout). We shall therefore calculate the SNR of a pseudo-pure state by transforming it to the corresponding ground state $|0 \dots 0\rangle\langle 0 \dots 0| - 2^{-N}$ (if need be), taking the partial trace over all but one of the spins, and multiplying the maximum eigenvalue of the result by 4.



[t]

Fig. 2. Negative base ten logarithm of the polarization P as a function of the logarithm of the ratio of the energy level spacing to $k_{\text{B}}T$ for a one (solid), four (dash), sixteen (dash-dot) and sixty-four (dot) spin pseudo-pure state obtained by cyclic averaging. For protons in a standard 500 MHz spectrometer at room temperature, $E/(k_{\text{B}}T) \approx P \sim 10^{-5}$ at equilibrium.

The maximum eigenvalue of the partial trace over all but one of the spins in a pseudo-pure state obtained by cyclic averaging, as in Eq. (50), is easily seen to be $N/(4(2^N - 1))$, which decays almost exponentially with the number of spins N . There is an additional factor of $\sqrt{2^N - 1}$ which comes from averaging over $2^N - 1$ experiments, and gives a net SNR of $N/(4\sqrt{2^N - 1})$ for the average. The exponential time requirements of cyclic averaging will nonetheless force one to average over smaller groups, with consequently smaller improvements in the SNR. In any case, the SNR declines superpolynomially with N . Figure 2 shows how the signal strength changes as a function of the ratio of the energy level spacing to $k_{\text{B}}T$, relative to the signal in a perfectly polarized sample, when the pseudo-pure state is obtained by cyclic averaging, for varying numbers of spins.

Because of the many possible variations on the ideas and the difficulty of analyzing all of them, it is not practical to present simple formulae for the SNR of the other methods of preparing pseudo-pure states. Further complexity is

added to the situation by the ability to combine the various methods above. A number of such combinations are given in Knill *et al.* [34], along with bounds on the SNR for each. In our laboratory we are developing a new method, again based on field gradients, which enables the sample to be divided into discrete volumes and separate unitary transformations to be applied to each. In principle, this permits multiple experiments to be performed, and their results added, in a single experiment, thereby performing an average over multiple experiments in constant time. This new method could also be used in a variety of combinations with existing methods.

It is nevertheless encouraging to observe that the SNR of the two-spin conditional and relative pseudo-pure states given in Eqs. (51) and (52) is 1/2 in both cases; this is exactly the decline in the ground state population of a two-spin system compared to a one-spin. In Eq. (51), we attain this “theoretical limit” because the expansion of the density operator consists of a single term conditioned on the state of a single ancilla; it is not possible to do as well with more spins. In Eq. (52), however, it is because such permutations are able to concentrate polarization in a subset of the spins. We have found this makes it possible to derive a two-spin pseudo-pure state from a six-spin equilibrium state with *no* loss of SNR, whereas a simplistic ground-state population argument implies we should lose at least 1/2. This may be seen by adding up the rows in the rearrangement of $\hat{\rho}_{\text{eq}}$ shown in Eq. (55) below, which corresponds taking the traces of the four 16×16 blocks along the diagonal, and yields **Diag**(48, -16, -16, -16).

$$\begin{aligned}
 \mathbf{Diag} (& 6, 4, 4, 4, 4, 4, 4, 2, 2, 2, 2, 2, 2, 2, 2, 2, & (55) \\
 & 0, 0, 0, 0, 0, 0, 0, 0, 0, 0, -2, -2, -2, -2, -4, -4, \\
 & 0, 0, 0, 0, 0, 0, 0, 0, 0, 0, -2, -2, -2, -2, -4, -4, \\
 & 2, 2, 2, 2, 2, 2, -2, -2, -2, -2, -2, -2, -2, -4, -4, -6)
 \end{aligned}$$

The partial trace over one of the two remaining spins then gives **Diag**(32, -32), which when divided by 128 (twice the partition function) yields $\frac{1}{2}\mathbf{I}_z$ as claimed.

A general algorithm has recently been given by Schulman & Vazirani [46] whereby one can “distill” an M -spin relative pure state from an ensemble of molecules each containing N spins. Starting from a uniform polarization of P , this algorithm yields M perfectly polarized spins providing $M/N \sim O(P^2)$, a result anticipated by earlier work in NMR which showed that the polarization of a single spin can be enhanced by at most a factor $O(\sqrt{N})$ [49]. Unfortunately, given that $P \approx 10^{-5}$ for protons at equilibrium in a standard 500 MHz spectrometer, a molecule with of order 10^{10} spins would be needed to prepare a perfectly polarized state on a single spin — which is in a pseudo-pure state at equilibrium!

The importance of Schulman and Vazirani’s algorithm thus lies in the fact that it shows that there is sufficient order in a typical NMR sample of 10^{20} spins at room temperatures to make it at least theoretically possible to perform quantum computations on of order 10^{10} spins.

One might hope that a more tractable algorithm, in terms of the absolute resources required, could be found by requiring only that it produce a *pseudo*-pure state with bounded SNR from the high-temperature equilibrium state. Since in the high-temperature approximation the largest element of the density matrix decays exponentially with the number of spins, it is clear that any such an algorithm must go beyond that approximation. Even so, given that Schulman and Vazirani’s algorithm is currently far beyond our ability to implement physically, it seems unlikely that a practical breakthrough will be obtained by purely algorithmic means. Fortunately, physical methods of “refrigerating” the spins are available, for example optical pumping [41]. These are presently confined to very simple systems, but such a source of polarization could in principle be used in conjunction with polarization transfer techniques to produce (pseudo-)pure states on large numbers of spins. Even at the low polarizations we can conveniently access, however, NMR has proved itself to be a powerful means of exploring quantum dynamics in Hilbert spaces of substantial size. To illustrate this, we will now present the results of NMR experiments which constitute a macroscopic analogue of a quantum mechanical test for quantum correlations that are inconsistent with the existence of “hidden variables”.

5 Macroscopic analogues of quantum correlations

Given the success of the purely classical Bloch equations (and their multispin extensions) in describing liquid-state NMR phenomena [19, 21, 40, 47], it is perhaps surprising that experiments can be performed whose mathematical description, at least, is formally identical to that of experiments which are believed to demonstrate uniquely “quantum” phenomena. For example, Seth Lloyd has recently proposed that the nonclassical correlations in (Mermin’s version of) the GHZ state can be validated using NMR [37]. His approach involves using a fourth “observer” spin to perform a nondemolition measurement on the three spins in a GHZ state (or a pseudo-pure analogue thereof). Here we shall describe experiments which demonstrate another, rather different way in which we can “emulate” quantum phenomena with liquid-state NMR. In reading this account,

it should be kept in mind that although pseudo-pure states do provide a faithful representation of the transformations of pure states within the highly mixed states that are available in liquid-state NMR, their physical interpretation differs significantly from that of true pure states. Hence, as discussed in greater detail at the end of this section (and also in Ref. [11]), our results should *not* be taken to resolve any foundational issues in quantum mechanics [43]. They demonstrate, nonetheless, a degree of coherent control sufficient to enable such issues to be addressed, *if* these same transformations and measurements were applied to a true pure state.

The approach taken here was inspired by an educational paper published a few years ago, in which T. F. Jordan has shown that the contradictions with hidden variables implied by violations of Bell’s inequalities as well as by the GHZ and Hardy’s paradox can be derived entirely by consideration of the expectation values of product operators, rather than by observations on single spins [33]. This shows that, in principle, it is not necessary to use nondemolition measurements with an observer spin in order to perform experiments which demonstrate these contradictions by NMR; it can be done directly from observations on ensembles of the spins of interest, providing at least they are in a (pseudo-)pure state. In a companion paper to Jordan’s, N. D. Mermin points out that in real-life experiments it is nevertheless not possible to perform the measurements, either of single spins nor (by implication) of expectation values, with sufficient precision to establish the “perfect” (total) correlations on which “EPR” arguments against the existence of hidden variables are based [39]. In that same paper, however, Mermin shows that Hardy’s paradox is a special case of the Clauser-Horne form of Bell’s inequality. This enables Hardy’s paradox [10, 26] to be extended to an open set in the Hilbert space of only two spins, to which sufficiently precise experimental data can confine us.

In the following, we present the results of NMR experiments which implement the specific example of Hardy’s paradox presented by Mermin in an Appendix to his paper [39]. Let us map the “red” and “green” eigenstates $|1\text{G}\rangle$ and $|1\text{R}\rangle$ of Mermin’s measurement 1 to the spin states $|0\rangle$ and $|1\rangle$, respectively. It will be clearer here to relabel this measurement as “A”, and to use $|\alpha_{\text{G}}\rangle \equiv |0\rangle$ and $|\alpha_{\text{R}}\rangle \equiv |1\rangle$ as synonyms for its eigenbasis. Correspondingly, we will relabel Mermin’s measurement 2 as “B”, and denote its the eigenbasis by

$$|\beta_{\text{G}}\rangle \equiv \sqrt{\frac{3}{5}}|0\rangle - \sqrt{\frac{2}{5}}|1\rangle \quad \text{and} \quad |\beta_{\text{R}}\rangle \equiv \sqrt{\frac{2}{5}}|0\rangle + \sqrt{\frac{3}{5}}|1\rangle. \quad (56)$$

Then the state which Mermin has shown leads to a near-maximum violation of

Bell's inequality while also providing an example of Hardy's paradox is

$$|\psi\rangle \equiv \frac{1}{2}|00\rangle + \sqrt{\frac{3}{8}}|01\rangle + \sqrt{\frac{3}{8}}|10\rangle. \quad (57)$$

To translate this into the context of NMR, we first note that the observable whose expectation value is the probability that measurement **A** yields the state $|\alpha_G\rangle$ is given by $\mathbf{A} \equiv \mathbf{E}_+ = \frac{1}{2}(1 + 2\mathbf{I}_z)$ (we drop the usual spin index because the measurements **A** & **B** are assumed the same for both spins). Similarly the observable which gives the probability that measurement **B** yields $|\beta_G\rangle$ is

$$\begin{aligned} \mathbf{B} &\equiv |\beta_G\rangle\langle\beta_G| = \frac{3}{5}|0\rangle\langle 0| + \frac{2}{5}|1\rangle\langle 1| - \sqrt{\frac{6}{25}}(|0\rangle\langle 1| + |1\rangle\langle 0|) \\ &= \frac{1}{2} + \frac{1}{5}\mathbf{I}_z - \sqrt{\frac{24}{25}}\mathbf{I}_x. \end{aligned} \quad (58)$$

In addition, the density operator (including the identity) of Mermin's state is

$$\begin{aligned} \Psi &\equiv |\psi\rangle\langle\psi| = \frac{1}{4} + \frac{1}{8}(\mathbf{I}_z^1 + \mathbf{I}_z^2) - \frac{1}{2}\mathbf{I}_z^1\mathbf{I}_z^2 \\ &\quad + \sqrt{\frac{3}{8}}(\mathbf{I}_x^1(1 + 2\mathbf{I}_z^2) + (1 + 2\mathbf{I}_z^1)\mathbf{I}_x^2) \\ &\quad + \frac{3}{4}(\mathbf{I}_x^1\mathbf{I}_x^2 + \mathbf{I}_y^1\mathbf{I}_y^2). \end{aligned} \quad (59)$$

The state $|01\rangle$ is obviously related to $|00\rangle$ by a rotation of spin 2, while $|00\rangle$ can likewise be rotated to $|10\rangle$, but without affecting $|01\rangle$, by a *conditional* rotation of spin 1. We shall denote these by

$$\mathbf{P}(\phi) \equiv e^{-i\phi\mathbf{I}_y^2} \quad \text{and} \quad \mathbf{Q}(\theta) \equiv e^{-i\theta\mathbf{I}_y^1\mathbf{E}_+^2}, \quad (60)$$

respectively. They act consecutively on the ground state to yield

$$\langle 00|\tilde{\mathbf{P}}(\phi)\tilde{\mathbf{Q}}(\theta) = [\cos(\theta/2)\cos(\phi/2), \sin(\theta/2)\cos(\phi/2), \sin(\phi/2), 0], \quad (61)$$

which is easily verified to equal $\langle\psi| = [1/2, \sqrt{3/8}, \sqrt{3/8}, 0]$ when

$$\phi = 2\arctan(\sqrt{3/5}) \quad \text{and} \quad \theta = 2\arctan(\sqrt{3/2}). \quad (62)$$

Using the product operator techniques presented in section 3, these transformations are readily implemented by NMR pulse sequences.

The next thing to notice is that if we take expectation values with the usual idempotents $\mathbf{E}_+^1\mathbf{E}_+^2, \dots, \mathbf{E}_-^1\mathbf{E}_-^2$, we get

$$\begin{aligned} \frac{1}{4} &= 4\langle\Psi\mathbf{E}_+^1\mathbf{E}_+^2\rangle \equiv 4\langle\Psi\mathbf{A}^1\mathbf{A}^2\rangle \\ \frac{3}{8} &= 4\langle\Psi\mathbf{E}_+^1\mathbf{E}_-^2\rangle \equiv 4\langle\Psi\mathbf{A}^1(1 - \mathbf{A}^2)\rangle \\ \frac{3}{8} &= 4\langle\Psi\mathbf{E}_-^1\mathbf{E}_+^2\rangle \equiv 4\langle\Psi(1 - \mathbf{A}^1)\mathbf{A}^2\rangle \\ 0 &= 4\langle\Psi\mathbf{E}_-^1\mathbf{E}_-^2\rangle \equiv 4\langle\Psi(1 - \mathbf{A}^1)(1 - \mathbf{A}^2)\rangle. \end{aligned} \quad (63)$$

These correspond to the diagonal of the density matrix in the usual \mathbf{I}_z basis,

$$\mathbf{diag}(\Psi) = [\frac{1}{4}, \frac{3}{8}, \frac{3}{8}, 0] \quad (\text{A on 1, A on 2}), \quad (64)$$

which contains the probabilities of the four possible outcomes of performing measurement A on both spins (as shown).

The product operator form of \mathbf{B} immediately makes clear that measurement B is just a measurement of the magnetization of the spin along an axis inclined at an angle of $\zeta \equiv \arctan(\sqrt{24}) = \pi - \theta$ to the z-axis in the xz-plane. Letting $\mathbf{R} \equiv \exp(-i\zeta\mathbf{I}_y)$, it follows that the probability that measurement B on spin 1 yields “G” (i.e. $|\beta_G\rangle$) is

$$4\langle \Psi \mathbf{B}^1 \rangle = 4\langle \Psi \tilde{\mathbf{R}}^1 \mathbf{A}^1 \mathbf{R}^1 \rangle = 4\langle \mathbf{R}^1 \Psi \tilde{\mathbf{R}}^1 \mathbf{A}^1 \rangle. \quad (65)$$

with a similar expression for spin 2. More generally, the probabilities of the outcomes of the other combinations of measurements are given by the diagonals of the transformed density matrices:

$$\begin{aligned} \mathbf{diag}(\mathbf{R}^2 \Psi \tilde{\mathbf{R}}^2) &= [0, \frac{5}{8}, \frac{9}{40}, \frac{3}{20}] && (\text{A on 1, B on 2}) \\ \mathbf{diag}(\mathbf{R}^1 \Psi \tilde{\mathbf{R}}^1) &= [0, \frac{9}{40}, \frac{5}{8}, \frac{3}{20}] && (\text{B on 1, A on 2}) \\ \mathbf{diag}(\mathbf{R}^1 \mathbf{R}^2 \Psi \tilde{\mathbf{R}}^2 \tilde{\mathbf{R}}^1) &= [\frac{9}{100}, \frac{27}{200}, \frac{27}{200}, \frac{16}{25}] && (\text{B on 1, B on 2}) \end{aligned} \quad (66)$$

For compactness, let us denote these probabilities by Ψ_{kl}^{ij} , where $i, j \in \{\mathbf{A}, \mathbf{B}\}$ are the measurements and $k, l \in \{\mathbf{G}, \mathbf{R}\}$ are the corresponding outcomes, e.g. $\Psi_{\mathbf{GR}}^{\mathbf{AB}} = 4\langle \Psi \mathbf{A}^1 (1 - \mathbf{B}^2) \rangle$.

We may translate Mermin’s proof [39] that these probabilities are incompatible with hidden variables associated with the individual spins into this context as follows: First, since $\Psi_{\mathbf{GG}}^{\mathbf{AB}} = \Psi_{\mathbf{GG}}^{\mathbf{BA}} = 0$, in any molecule wherein one of the spins is parallel to the z-axis the other must be antiparallel to the axis of measurement B and vice versa. Hence, since $\Psi_{\mathbf{GG}}^{\mathbf{BB}}$ is nonzero, in some molecules (9%, to be precise) both spins must be antiparallel to the z-axis. But this contradicts the fact that $\Psi_{\mathbf{RR}}^{\mathbf{AA}} = 0$. More generally, Mermin has shown that

$$\Psi_{\mathbf{GG}}^{\mathbf{BB}} \leq \Psi_{\mathbf{GG}}^{\mathbf{AB}} + \Psi_{\mathbf{RR}}^{\mathbf{AA}} + \Psi_{\mathbf{GG}}^{\mathbf{BA}} \quad (67)$$

is an example of the Clauser-Horne form of Bell’s inequality [43]. Hence to disprove the existence of such one-particle hidden variables it would be sufficient to determine these probabilities to $\pm 2\%$ or so.

At this point we encounter a significant complication, which is that the “strong” (von Neumann) measurements assumed in their analyses by Jordan and Mermin *cannot* be implemented by NMR; we can only perform “weak”

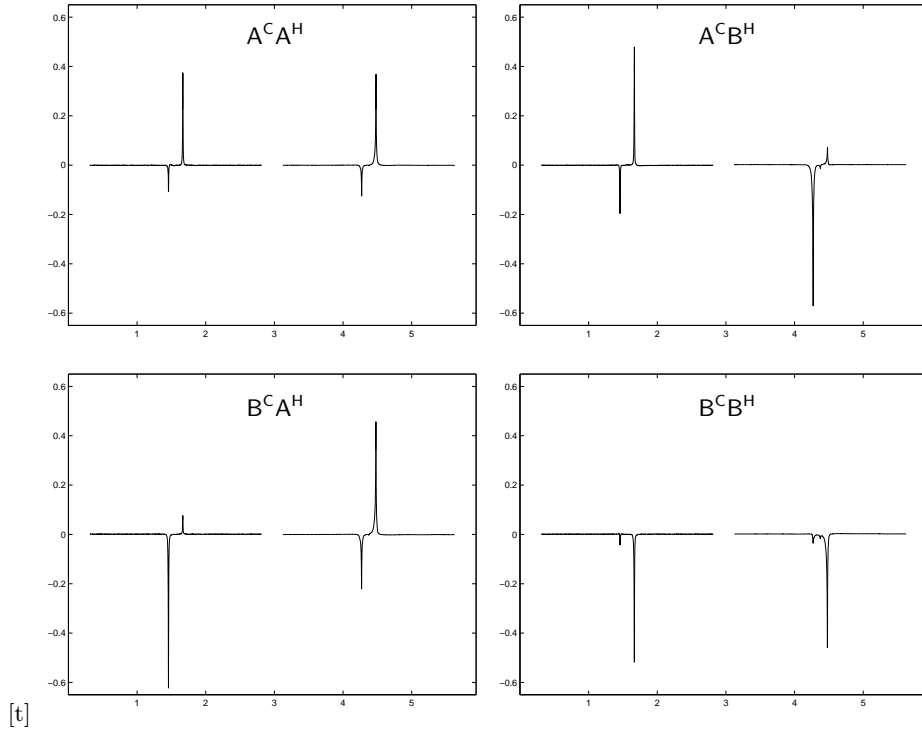


Fig. 3. The pairs of ^{13}C -labeled chloroform (CHCl_3) spectra (carbon left, proton right) obtained by performing the four combinations of measurements $A^C A^H$, $A^C B^H$, $B^C A^H$ and $B^C B^H$ on the pseudo-pure form of Mermin's state Ψ . The spectra have been normalized by the height of the peak of the corresponding spin in the pseudo-pure ground state, and the horizontal axis is in kHz. The transitions of the peaks, from left to right, are $|0^C 0^H\rangle \leftrightarrow |1^C 0^H\rangle$, $|0^C 1^H\rangle \leftrightarrow |1^C 1^H\rangle$, $|0^C 0^H\rangle \leftrightarrow |0^C 1^H\rangle$, $|1^C 0^H\rangle \leftrightarrow |1^C 1^H\rangle$.

Probabilities of Outcomes G & R for the Measurements A & B (Carbon, Proton) Demonstrating Hardy's Paradox, as Derived from the Chloroform NMR Spectra in Fig. 3					
Measurements	(G, G)	(G, R)	(R, G)	(R, R)	Residuals
(A^C, A^H)	0.253	0.380	0.366	0.001	0.008
(A^C, B^H)	0.029	0.609	0.217	0.145	0.018
(B^C, A^H)	-0.002	0.230	0.614	0.159	0.005
(B^C, B^H)	0.097	0.125	0.156	0.622	0.021

(nonperturbing) measurements of the *probability differences* between states connected by single spin flips [16]. This is done by applying a magnetic field gradient along the z-axis, which (as previously described) dephases any transverse components in the density operator. Thereafter, a pair of “soft” $\pi/2$ readout pulses, each tuned to the frequency of just one of the two spins, produces a pair of spectra each with two peaks whose heights are proportional to the probability differences between pairs of states connected by flips of that spin. The factor relating the peak heights to the corresponding differences in the probabilities of the states can be determined from spectra collected on the pseudo-pure ground state, after which it is straightforward to convert the differences into the corresponding absolute probabilities by linear least squares, subject to the constraint that their sum is unity. We shall encounter field gradients again in the next section, when we show how they can also be used to implement precisely controlled decoherence models.

Thus the overall experiment consists of collecting ten spectra, as follows:

1. Prepare the state Ψ , by first preparing the pseudo-pure ground state $|00\rangle$ using one of the previously described methods, and then transforming it by $\mathbf{Q}(\theta)\mathbf{P}(\phi)$.
2. Use a selective radio-frequency pulse to apply the rotation \mathbf{R} to those spins on which measurement \mathbf{B} is to be performed.
3. Use a z-gradient to dephase the transverse components of the resulting density operator.
4. Apply a readout pulse to one of the spins, and collect the corresponding spectrum; repeat steps 1 – 3 and then do the same for the other spin.
5. Repeat steps 1 - 4 for each of the four combinations of measurements AA, AB, BA and BB on the two spins.
6. Collect two additional amplitude calibration spectra by applying soft readout pulses to each spin in the pseudo-pure ground state.

These experiments were performed on a Bruker 400 MHz spectrometer using the two spin $\frac{1}{2}$ nuclei in ^{13}C -labeled chloroform.

The spectra obtained from steps 1 – 5 of this experiment are shown in Fig. 3. The probabilities derived from these peak heights, and the residual (square-root of the sum of squares of the deviations of the data points from the corresponding fit) associated with each, are shown in the table below. It follows that Bell’s

inequality is violated by

$$\begin{aligned} & \psi_{GG}^{AB} + \psi_{RR}^{AA} + \psi_{GG}^{BA} - \psi_{GG}^{BB} \\ &= 0.029 + 0.001 - 0.002 - 0.097 = -0.069 . \end{aligned} \tag{68}$$

A rigorous error analysis is not possible, because the dominant errors in NMR spectra (e.g. RF field inhomogeneity) are not statistical. If we nevertheless take the mean RMS residual (half the total residuals shown in the table) of 0.0065 as an estimate of the errors and assume they are independent between spectra, the expected error in the sum of these four numbers is only 0.013, so that this violation of Bell’s inequality appears significant.

Nonetheless, as stressed in a recent preprint by Braunstein, Caves, Jozsa, Linden, Popescu and Schack [11], such experiments on weakly polarized pseudo-pure states cannot actually disprove the existence of “hidden variables” associated with the spins of the individual molecules. This is because the vast majority of a weakly polarized density operator is contained in its identity component, and there are many different ensembles of uncorrelated spin states whose net density operator is the identity. Hence the noise from the identity component dominates the statistics of observations on the ensemble, which are therefore consistent with microscopic interpretations in which only uncorrelated states are present with nonzero probability. Indeed, if one were to pull the molecules out the pseudo-pure sample used in the above experiments one at a time, break them apart, and perform the measurements A and B with a Stern-Gerlach apparatus, the frequencies of the four combinations of outcomes would all be very close to 1/4, and would *not* violate Bell’s inequality. Thus, our apparent violation vanishes when the whole ensemble is taken into consideration.

To see more precisely why the above experiments fail to disprove the existence of hidden variables, we first note that a pure state $|\xi\rangle\langle\xi|$ is canonically associated with any given pseudo-pure density operator $\rho = (1 - \delta)/2^N + \delta |\xi\rangle\langle\xi|$, which is distinguished mathematically by the fact that $|\xi\rangle$ is the eigenvector corresponding to its *sole* nondegenerate eigenvalue. We further recall (see Eq. (44)) that the traceless part of the pseudo-pure density operator ρ transforms identically to that of the corresponding pure state $|\xi\rangle\langle\xi|$ under unitary operations, while the identity component transforms trivially, and also that ρ produces exactly the same NMR spectrum as would $|\xi\rangle\langle\xi|$ up to its overall amplitude (since the identity component of any density operator does not contribute to the signals observed by NMR). Thus the unitary dynamics of the observables in NMR experiments on pseudo-pure states are, for all practical intents and pur-

poses, indistinguishable from the same experiments on a (smaller) ensemble in the corresponding pure state $|\xi\rangle\langle\xi|$.

It follows that NMR experiments on pseudo-pure states are necessarily *consistent with* (though not proof of the reality of) a microscopic interpretation of the ensemble in which those molecules contributing to the observations are all in the same pure state $|\xi\rangle\langle\xi|$, while the remaining (and large majority of the) molecules are in completely random states with a net density operator of $1/2^N$. In deriving a violation of Bell’s inequality from our measurements above, we required that the fractions of molecules in the four diagonal states sum to unity, so that they could be identified with the probabilities of those states in an unidentified subensemble in the pure state $|\psi\rangle\langle\psi|$. Implicitly, therefore, this microscopic interpretation of the ensemble was assumed in deriving the violation. As explained above, however, the large identity component in the corresponding pseudo-pure density operator guarantees that many other ensembles could be found with the same net density operator, so that a microscopic interpretation in terms of a single well-defined subensemble in the pure state $|\psi\rangle\langle\psi|$ is not physically justified. In fact, the fundamental limits on the amount of information that can be extracted on an unknown quantum state even by strong measurements prevents us from ever knowing if any molecules of our pseudo-pure sample exist in or near the corresponding pure state $|\psi\rangle\langle\psi|$ at all [43]. It is for this reason that our apparent violation of Bell’s inequality fails to disprove the existence of hidden variables.

This ambiguity in the microscopic interpretation of liquid-state NMR experiments not-with-standing, quantum physics indicates that a pseudo-pure spin state, subjected to the same electromagnetic fields as a true pure state, will undergo the same unitary transformation. In addition, applying a z-gradient to an NMR ensemble renders unobservable the same transverse phase information that would be destroyed on performing strong measurements along the z-axis on all the spins in the ensemble. Finally, existing experiments relying upon true pure states and strong measurements provide direct evidence against hidden variable theories (see e.g. Ref. [2, 10]). Given this background knowledge of the underlying physics, our experiments indirectly imply that the pure state $|\psi\rangle\langle\psi|$ would violate Bell’s inequality. More generally, the ambiguity in the microscopic interpretation of liquid-state NMR experiments in *no way* detracts from their utility as a means of studying the dynamics of information contained in either pseudo-pure or (by inference) true pure states, even in significantly more complex spin systems that would be difficult to study by other means. To further emphasize this fact, we will now describe NMR experiments we have performed

which demonstrate quantum error correction using pseudo-pure states.

6 Quantum error correction by NMR spectroscopy

The error correcting code we have chosen to illustrate by NMR is well-known in the field [35], and uses two ancilla (labeled 2 & 3) to encode the state of a data spin (labeled 1). Letting $\mathbf{S}^{2|1}$ and $\mathbf{S}^{3|1}$ be c-NOT's, and $\mathbf{R}_{90}^{123} \equiv \exp(-i\frac{\pi}{2}(\mathbf{I}_y^1 + \mathbf{I}_y^2 + \mathbf{I}_y^3))$, the encoding operation proceeds as follows:

$$\begin{aligned} & (\alpha|0\rangle + \beta|1\rangle)|00\rangle/\sqrt{2} \xrightarrow{\mathbf{S}^{2|1}} \xrightarrow{\mathbf{S}^{3|1}} \xrightarrow{\mathbf{R}_{90}^{123}} \alpha|+++ \rangle + \beta|--- \rangle \\ & \text{(where } |\pm\pm\pm\rangle \equiv (|0\rangle \pm |1\rangle)(|0\rangle \pm |1\rangle)(|0\rangle \pm |1\rangle)/\sqrt{8}) \end{aligned} \quad (69)$$

Decoding consists of applying the inverse operations in the reverse order, which acts on the states obtained by single sign-flip errors as follows:

$$\begin{aligned} & \alpha|++- \rangle + \beta|--+ \rangle \xrightarrow{\mathbf{R}_{-90}^{123}} \xrightarrow{\mathbf{S}^{3|1}} \xrightarrow{\mathbf{S}^{2|1}} (\alpha|0\rangle + \beta|1\rangle)|01\rangle/\sqrt{2} \\ & \alpha|+-+ \rangle + \beta|-+- \rangle \xrightarrow{\mathbf{R}_{-90}^{123}} \xrightarrow{\mathbf{S}^{3|1}} \xrightarrow{\mathbf{S}^{2|1}} (\alpha|0\rangle + \beta|1\rangle)|10\rangle/\sqrt{2} \\ & \alpha|-++ \rangle + \beta|+-- \rangle \xrightarrow{\mathbf{R}_{-90}^{123}} \xrightarrow{\mathbf{S}^{3|1}} \xrightarrow{\mathbf{S}^{2|1}} (\alpha|1\rangle + \beta|0\rangle)|11\rangle/\sqrt{2} \end{aligned} \quad (70)$$

It follows that a Toffoli gate $\mathbf{T}^{1|23}$, which flips the data spin conditional on the ancillae being in the state $|11\rangle$, will correct a sign-flip error in the data spin and leave it alone otherwise, even if an error occurs in the ancillae.

In practice, errors in quantum computers are not expected to be single sign-flips, but rather small random phase errors which cumulatively result in decoherence. Nevertheless, we can show that the ability to correct sign-flips implies the ability to cancel the effect of such phase errors to first order. Random phase errors correspond to the propagator $\exp(-i(\chi^1\mathbf{I}_z^1 + \chi^2\mathbf{I}_z^2 + \chi^3\mathbf{I}_z^3))$, where χ^1, χ^2, χ^3 are random variables, which acts to first order on the encoded state as:

$$\begin{aligned} & \exp(-i(\chi^1\mathbf{I}_z^1 + \chi^2\mathbf{I}_z^2 + \chi^3\mathbf{I}_z^3)) (\alpha|+++ \rangle + \beta|--- \rangle) \\ & \approx (\alpha|+++ \rangle + \beta|--- \rangle) - i\chi^1 (\alpha|-++ \rangle + \beta|+-- \rangle) \\ & \quad - i\chi^2 (\alpha|+-+ \rangle + \beta|-+- \rangle) - i\chi^3 (\alpha|++- \rangle + \beta|--+ \rangle) \end{aligned} \quad (71)$$

Since decoding and the error-correcting Toffoli gate are likewise linear, it follows that the first-order effects of phase errors are cancelled as claimed. Note this argument makes no assumptions concerning the correlations among the errors!

Experimental results demonstrating these expectations have recently been published [15]. In the following, we shall present a more detailed explanation of how the error correction works using the product operator formalism, along with selected experimental data illustrating and validating this explanation. We shall assume that the data spin is in one of the states 1 (unpolarized), \mathbf{I}_x^1 , \mathbf{I}_y^1 or \mathbf{I}_z^1 . Although these are mixed states, each consists of an incoherent sum of pure states, e.g. $2\mathbf{I}_z^1 = |0\rangle\langle 0| - |1\rangle\langle 1|$, so if error correction works on these pure states, by linearity it will also work on the mixtures (and vice versa). In these terms, a complete set of initial states ρ_A for error correction are:

$$\left. \begin{array}{l} \mathbf{E}_+^2 \mathbf{E}_+^3 \\ \mathbf{I}_x^1 \mathbf{E}_+^2 \mathbf{E}_+^3 \\ \mathbf{I}_y^1 \mathbf{E}_+^2 \mathbf{E}_+^3 \\ \mathbf{I}_z^1 \mathbf{E}_+^2 \mathbf{E}_+^3 \end{array} \right\} \equiv \rho_A^1 \mathbf{E}_+^2 \mathbf{E}_+^3 = \rho_A \quad (72)$$

The corresponding states ρ_B to which they are mapped by encoding are:

$$\rho_B \equiv \begin{cases} \frac{1}{4} + \mathbf{I}_x^1 \mathbf{I}_x^2 + \mathbf{I}_x^1 \mathbf{I}_x^3 + \mathbf{I}_x^2 \mathbf{I}_x^3 \\ \mathbf{I}_z^1 \mathbf{I}_y^2 \mathbf{I}_y^3 + \mathbf{I}_y^1 \mathbf{I}_z^2 \mathbf{I}_z^3 + \mathbf{I}_y^1 \mathbf{I}_y^2 \mathbf{I}_z^3 - \mathbf{I}_z^1 \mathbf{I}_z^2 \mathbf{I}_z^3 \\ \mathbf{I}_z^1 \mathbf{I}_z^2 \mathbf{I}_y^3 + \mathbf{I}_z^1 \mathbf{I}_y^2 \mathbf{I}_z^3 + \mathbf{I}_y^1 \mathbf{I}_z^2 \mathbf{I}_z^3 - \mathbf{I}_y^1 \mathbf{I}_y^2 \mathbf{I}_y^3 \\ \frac{1}{4}(\mathbf{I}_x^1 + \mathbf{I}_x^2 + \mathbf{I}_x^3) + \mathbf{I}_x^1 \mathbf{I}_x^2 \mathbf{I}_x^3 \end{cases} \quad (73)$$

We note the last three states in Eq. (72) can be prepared (with a 50% loss of polarization) from the average of twice Eq. (51) with

$$\begin{aligned} & \frac{1}{16} \mathbf{Diag}(3, 1, 1, 1, -3, -1, -1, -1) \\ \leftrightarrow & \frac{1}{16}(\mathbf{I}_z^1(3 + 2\mathbf{I}_z^2 + 2\mathbf{I}_z^3 + 4\mathbf{I}_z^2 \mathbf{I}_z^3)) \\ = & \frac{1}{4}(\mathbf{E}_+^1 - \mathbf{E}_-^1)(\mathbf{E}_+^2 \mathbf{E}_+^3 + \frac{1}{2}). \end{aligned} \quad (74)$$

In liquid-state NMR, decoherence occurs principally through the randomly fluctuating external magnetic fields B_z^k along the z-axis at each spin k . The effect of these fields is most simply described in the *spherical* product operator basis $\mathbf{1}$, \mathbf{I}_z^k and $\mathbf{I}_\pm^k \equiv \mathbf{I}_x^k \pm i\mathbf{I}_y^k$, as opposed to the *Cartesian* basis used up to now. The products of these basis elements can be shown [19] to decay exponentially at rates proportional to the mean-square field $\overline{(B_z^k)^2}$ for \mathbf{I}_\pm^k (as well as $\mathbf{I}_\pm^k \mathbf{I}_z^\ell$,

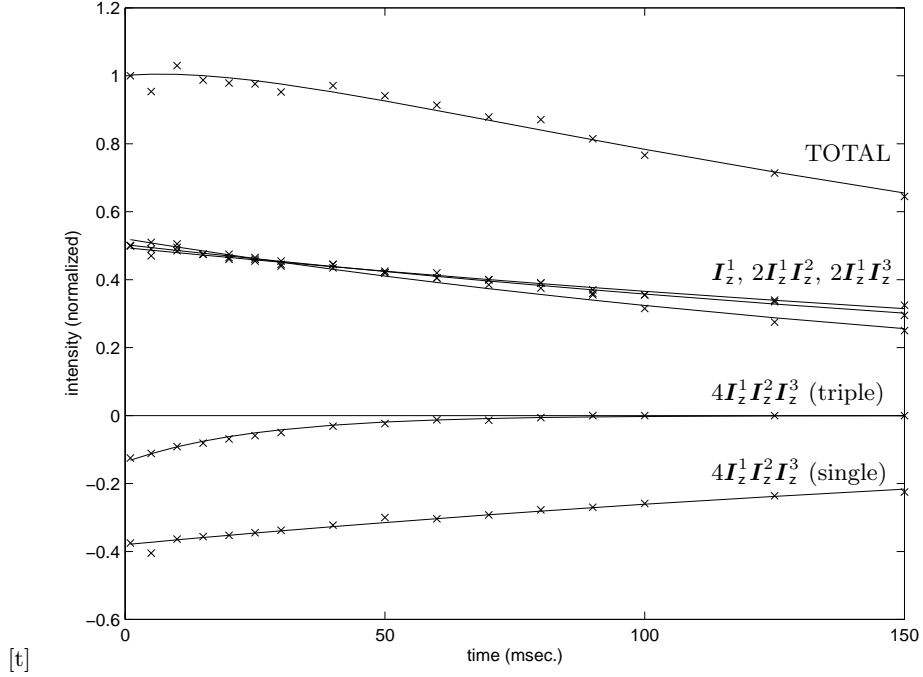


Fig. 4. Experimental NMR data illustrating the decay of each of the product operators I_z^1 , $2I_z^1 I_z^2$, $2I_z^1 I_z^3$, $4I_z^1 I_z^2 I_z^3$, as functions of the time allowed for gradient diffusion (see text), together with the least-squares fits to their logarithms. The single and triple quantum coherences in $4I_z^1 I_z^2 I_z^3$, (negative curves) have been plotted and fit separately. The sum of these data and of the fits are also shown (topmost curve), which illustrates that error correction cancels the decay of the encoded state to first order as expected.

$I_{\pm}^k I_z^{\ell} I_z^m$), and to

$$\begin{aligned}
 & \overline{(B_z^k - B_z^{\ell})^2} && \text{for } I_+^k I_-^{\ell} \text{ \& } I_-^k I_+^{\ell}, && (75) \\
 & \overline{(B_z^k + B_z^{\ell})^2} && \text{for } I_+^k I_+^{\ell} \text{ \& } I_-^k I_-^{\ell}, \\
 & \overline{(B_z^k + B_z^{\ell} - B_z^m)^2} && \text{for } I_+^k I_+^{\ell} I_-^m \text{ \& } I_-^k I_-^{\ell} I_+^m, \text{ etc.,} \\
 \text{and } & \overline{(B_z^k + B_z^{\ell} + B_z^m)^2} && \text{for } I_+^k I_+^{\ell} I_+^m \text{ \& } I_-^k I_-^{\ell} I_-^m.
 \end{aligned}$$

These products are referred to as single (SQC1: I_{\pm}^k), zero (ZQC: $I_{\pm}^k I_{\mp}^{\ell}$), double (DQC: $I_{\pm}^k I_{\pm}^{\ell}$), three-spin single (SQC3: $I_{\pm}^k I_{\pm}^{\ell} I_{\mp}^m$, etc.) and triple (TQC: $I_{\pm}^k I_{\pm}^{\ell} I_{\pm}^m$) quantum coherences, respectively.

We shall consider two extreme forms of decoherence. In the first, the fields at the different spins are uncorrelated, and hence the random variables χ^k can be assumed to be identically distributed and independent. In the second, they are

assumed to be totally correlated. By Eq. (75), the relative rates of decoherence in these two cases are:

	ZQC	SQC1	SQC3	DQC	TQC	
Uncorrelated:	2	1	3	2	3	(76)
Totally Correlated:	0	1	1	4	9	

Decomposing $\rho_{\mathbf{B}}$ into a spherical basis, multiplying by decaying exponentials with the above rates normalized by the SQC1 decay rate τ , and returning to the Cartesian basis gives

$$\rho_{\mathbf{C}} \equiv \begin{cases} \frac{1}{4} + (\mathbf{I}_x^1 \mathbf{I}_x^2 + \mathbf{I}_x^1 \mathbf{I}_x^3 + \mathbf{I}_x^2 \mathbf{I}_x^3) e^{-2t/\tau} \\ (\mathbf{I}_z^1 \mathbf{I}_y^2 \mathbf{I}_y^3 + \mathbf{I}_y^1 \mathbf{I}_z^2 \mathbf{I}_y^3 + \mathbf{I}_y^1 \mathbf{I}_y^2 \mathbf{I}_z^3) e^{-2t/\tau} - \mathbf{I}_z^1 \mathbf{I}_z^2 \mathbf{I}_z^3 \\ (\mathbf{I}_z^1 \mathbf{I}_z^2 \mathbf{I}_y^3 + \mathbf{I}_z^1 \mathbf{I}_y^2 \mathbf{I}_z^3 + \mathbf{I}_y^1 \mathbf{I}_z^2 \mathbf{I}_z^3) e^{-t/\tau} - \mathbf{I}_y^1 \mathbf{I}_y^2 \mathbf{I}_y^3 e^{-3t/\tau} \\ \frac{1}{4} (\mathbf{I}_x^1 + \mathbf{I}_x^2 + \mathbf{I}_x^3) e^{-t/\tau} + \mathbf{I}_x^1 \mathbf{I}_x^2 \mathbf{I}_x^3 e^{-3t/\tau} \end{cases} \quad (77)$$

in the uncorrelated case, and

$$\rho_{\mathbf{C}} \equiv \begin{cases} \frac{1}{4} + \frac{1}{2} (\mathbf{I}_x^1 \mathbf{I}_x^2 + \mathbf{I}_x^1 \mathbf{I}_x^3 + \mathbf{I}_x^2 \mathbf{I}_x^3 + \mathbf{I}_y^1 \mathbf{I}_y^2 + \mathbf{I}_y^1 \mathbf{I}_y^3 + \mathbf{I}_y^2 \mathbf{I}_y^3) \\ + \frac{1}{2} (\mathbf{I}_x^1 \mathbf{I}_x^2 + \mathbf{I}_x^1 \mathbf{I}_x^3 + \mathbf{I}_x^2 \mathbf{I}_x^3 - \mathbf{I}_y^1 \mathbf{I}_y^2 - \mathbf{I}_y^1 \mathbf{I}_y^3 - \mathbf{I}_y^2 \mathbf{I}_y^3) e^{-4t/\tau} \\ \frac{1}{2} (\mathbf{I}_z^1 (\mathbf{I}_x^2 \mathbf{I}_x^3 + \mathbf{I}_y^2 \mathbf{I}_y^3) + \mathbf{I}_z^2 (\mathbf{I}_x^1 \mathbf{I}_x^3 + \mathbf{I}_y^1 \mathbf{I}_y^3) + \mathbf{I}_z^3 (\mathbf{I}_x^1 \mathbf{I}_x^2 + \mathbf{I}_y^1 \mathbf{I}_y^2)) \\ - \frac{1}{2} (\mathbf{I}_z^1 (\mathbf{I}_x^2 \mathbf{I}_x^3 - \mathbf{I}_y^2 \mathbf{I}_y^3) + \mathbf{I}_z^2 (\mathbf{I}_x^1 \mathbf{I}_x^3 - \mathbf{I}_y^1 \mathbf{I}_y^3) + \mathbf{I}_z^3 (\mathbf{I}_x^1 \mathbf{I}_x^2 - \mathbf{I}_y^1 \mathbf{I}_y^2)) \\ e^{-4t/\tau} - \mathbf{I}_z^1 \mathbf{I}_z^2 \mathbf{I}_z^3 \\ (\mathbf{I}_z^1 \mathbf{I}_z^2 \mathbf{I}_y^3 + \mathbf{I}_z^1 \mathbf{I}_y^2 \mathbf{I}_z^3 + \mathbf{I}_y^1 \mathbf{I}_z^2 \mathbf{I}_z^3) e^{-t/\tau} \\ + \frac{1}{4} (\mathbf{I}_x^1 \mathbf{I}_x^2 \mathbf{I}_y^3 + \mathbf{I}_x^1 \mathbf{I}_y^2 \mathbf{I}_x^3 + \mathbf{I}_y^1 \mathbf{I}_x^2 \mathbf{I}_x^3 + 3 \mathbf{I}_y^1 \mathbf{I}_y^2 \mathbf{I}_y^3) e^{-t/\tau} \\ - \frac{1}{4} (\mathbf{I}_x^1 \mathbf{I}_x^2 \mathbf{I}_y^3 + \mathbf{I}_x^1 \mathbf{I}_y^2 \mathbf{I}_x^3 + \mathbf{I}_y^1 \mathbf{I}_x^2 \mathbf{I}_x^3 - \mathbf{I}_y^1 \mathbf{I}_y^2 \mathbf{I}_y^3) e^{-9t/\tau} \\ \frac{1}{4} (\mathbf{I}_x^1 + \mathbf{I}_x^2 + \mathbf{I}_x^3) e^{-t/\tau} \\ + \frac{1}{4} (3 \mathbf{I}_x^1 \mathbf{I}_x^2 \mathbf{I}_x^3 + \mathbf{I}_y^1 \mathbf{I}_y^2 \mathbf{I}_x^3 + \mathbf{I}_y^1 \mathbf{I}_x^2 \mathbf{I}_y^3 + \mathbf{I}_x^1 \mathbf{I}_y^2 \mathbf{I}_y^3) e^{-t/\tau} \\ + \frac{1}{4} (\mathbf{I}_x^1 \mathbf{I}_x^2 \mathbf{I}_x^3 - \mathbf{I}_y^1 \mathbf{I}_y^2 \mathbf{I}_x^3 - \mathbf{I}_y^1 \mathbf{I}_x^2 \mathbf{I}_y^3 - \mathbf{I}_x^1 \mathbf{I}_y^2 \mathbf{I}_y^3) e^{-9t/\tau} \end{cases} \quad (78)$$

in the totally correlated case. The decoding operation converts this to

$$\rho_{\text{D}} \equiv \begin{cases} \frac{1}{4} + (\mathbf{I}_z^2 + \mathbf{I}_z^3 + \mathbf{I}_z^2 \mathbf{I}_z^3) e^{-2t/\tau} \\ (\frac{1}{2} \mathbf{I}_x^1 \mathbf{I}_z^2 + \frac{1}{2} \mathbf{I}_x^1 \mathbf{I}_z^3 + \mathbf{I}_x^1 \mathbf{I}_z^2 \mathbf{I}_z^3) e^{-2t/\tau} + \frac{1}{4} \mathbf{I}_x^1 \\ (\frac{1}{4} \mathbf{I}_y^1 + \frac{1}{2} \mathbf{I}_y^1 \mathbf{I}_z^2 + \frac{1}{2} \mathbf{I}_y^1 \mathbf{I}_z^3) e^{-t/\tau} + \mathbf{I}_y^1 \mathbf{I}_z^2 \mathbf{I}_z^3 e^{-3t/\tau} \\ (\frac{1}{4} \mathbf{I}_z^1 + \frac{1}{2} \mathbf{I}_z^1 \mathbf{I}_z^2 + \frac{1}{2} \mathbf{I}_z^1 \mathbf{I}_z^3) e^{-t/\tau} + \mathbf{I}_z^1 \mathbf{I}_z^2 \mathbf{I}_z^3 e^{-3t/\tau} \end{cases} \quad (79)$$

in the uncorrelated case, and

$$\rho_{\text{D}} \equiv \begin{cases} \frac{1}{4} + \frac{1}{2} (\frac{1}{2} \mathbf{I}_z^2 + \frac{1}{2} \mathbf{I}_z^3 + \mathbf{I}_z^2 \mathbf{I}_z^3 - 2 \mathbf{I}_x^1 \mathbf{I}_z^2 \mathbf{I}_y^3 - 2 \mathbf{I}_x^1 \mathbf{I}_y^2 \mathbf{I}_z^3 + \mathbf{I}_y^2 \mathbf{I}_y^3) \\ + \frac{1}{2} (\frac{1}{2} \mathbf{I}_z^2 + \frac{1}{2} \mathbf{I}_z^3 + \mathbf{I}_z^2 \mathbf{I}_z^3 + 2 \mathbf{I}_x^1 \mathbf{I}_z^2 \mathbf{I}_y^3 + 2 \mathbf{I}_x^1 \mathbf{I}_y^2 \mathbf{I}_z^3 - \mathbf{I}_y^2 \mathbf{I}_y^3) e^{-4t/\tau} \\ \frac{1}{2} (\mathbf{I}_x^1 (\mathbf{I}_y^2 \mathbf{I}_y^3 + \mathbf{I}_z^2 \mathbf{I}_z^3) + \frac{1}{2} \mathbf{I}_z^3 (\mathbf{I}_x^1 - \mathbf{I}_x^2) + \frac{1}{2} \mathbf{I}_z^2 (\mathbf{I}_x^1 - \mathbf{I}_x^3)) + \frac{1}{4} \mathbf{I}_x^1 \\ + \frac{1}{2} (\mathbf{I}_x^1 (\mathbf{I}_y^2 \mathbf{I}_y^3 - \mathbf{I}_z^2 \mathbf{I}_z^3) + \frac{1}{2} \mathbf{I}_z^3 (\mathbf{I}_x^1 + \mathbf{I}_x^2) + \frac{1}{2} \mathbf{I}_z^2 (\mathbf{I}_x^1 + \mathbf{I}_x^3)) e^{-4t/\tau} \\ (\frac{1}{2} \mathbf{I}_y^1 \mathbf{I}_z^3 + \frac{1}{2} \mathbf{I}_y^1 \mathbf{I}_z^2 + \frac{1}{4} \mathbf{I}_y^1) e^{-t/\tau} \\ + \frac{1}{4} (\mathbf{I}_z^1 \mathbf{I}_z^2 \mathbf{I}_y^3 + \mathbf{I}_z^1 \mathbf{I}_y^2 \mathbf{I}_z^3 - \mathbf{I}_y^1 \mathbf{I}_y^2 \mathbf{I}_y^3 - 3 \mathbf{I}_y^1 \mathbf{I}_z^2 \mathbf{I}_z^3) e^{-t/\tau} \\ - \frac{1}{4} (\mathbf{I}_z^1 \mathbf{I}_z^2 \mathbf{I}_y^3 + \mathbf{I}_z^1 \mathbf{I}_y^2 \mathbf{I}_z^3 - \mathbf{I}_y^1 \mathbf{I}_y^2 \mathbf{I}_y^3 + \mathbf{I}_y^1 \mathbf{I}_z^2 \mathbf{I}_z^3) e^{-9t/\tau} \\ \frac{1}{4} (\mathbf{I}_z^1 + 2 \mathbf{I}_z^1 \mathbf{I}_z^2 + 2 \mathbf{I}_z^1 \mathbf{I}_z^3) e^{-t/\tau} \\ + \frac{1}{4} (3 \mathbf{I}_z^1 \mathbf{I}_z^2 \mathbf{I}_z^3 + \mathbf{I}_y^1 \mathbf{I}_y^2 \mathbf{I}_z^3 + \mathbf{I}_y^1 \mathbf{I}_z^2 \mathbf{I}_y^3 + \mathbf{I}_z^1 \mathbf{I}_y^2 \mathbf{I}_y^3) e^{-t/\tau} \\ + \frac{1}{4} (\mathbf{I}_z^1 \mathbf{I}_z^2 \mathbf{I}_z^3 - \mathbf{I}_y^1 \mathbf{I}_y^2 \mathbf{I}_z^3 - \mathbf{I}_y^1 \mathbf{I}_z^2 \mathbf{I}_y^3 - \mathbf{I}_z^1 \mathbf{I}_y^2 \mathbf{I}_y^3) e^{-9t/\tau} \end{cases} \quad (80)$$

in the totally correlated case. This is clearly getting a little messy, and it gets much worse after the Toffoli gate! Therefore, we shall only present the partial trace over the ancillae after applying the Toffoli, which is

$$\rho_{\text{E}}^1 \equiv \begin{cases} 1 \\ \mathbf{I}_x^1 \\ \mathbf{I}_y^1 \left(\frac{3}{2} e^{-t/\tau} - \frac{1}{2} e^{-3t/\tau} \right) \\ \mathbf{I}_z^1 \left(\frac{3}{2} e^{-t/\tau} - \frac{1}{2} e^{-3t/\tau} \right) \end{cases} \quad (81)$$

in the uncorrelated case, and

$$\rho_{\text{E}}^1 \equiv \begin{cases} 1 \\ \mathbf{I}_x^1 \\ \mathbf{I}_y^1 \left(\frac{3}{2}e^{-t/\tau} - \frac{3}{8}e^{-t/\tau} - \frac{1}{8}e^{-9t/\tau} \right) \\ \mathbf{I}_z^1 \left(\frac{3}{2}e^{-t/\tau} - \frac{3}{8}e^{-t/\tau} - \frac{1}{8}e^{-9t/\tau} \right) \end{cases} \quad (82)$$

in the correlated. The slope of these curves at $t = 0$ is zero in all cases, as expected.

In order to demonstrate these results by NMR solution-state spectroscopy, a precise implementation of the above decoherence models is needed. This was achieved by combining *gradient* methods with molecular diffusion. In these methods, a magnetic field gradient is created along the z -axis; as previously described, this dephases the transverse (xy) magnetization. More precisely, a field gradient causes the transverse magnetization to precess at rates which depend linearly on its z -coordinate, thereby winding it into a spiral about the z -axis whose average transverse magnetization is essentially zero. The gradient is turned off for a given time interval t , during which diffusion of the molecules along z blurs the spiral. The gradient is then reversed, causing the magnetization to refocus and so create an “echo”. Because those molecules which have moved now precess at a different rate, their magnetization is not refocused, so the magnitude of the echo decays exponentially with t . Because all the spins in each molecule are subject to the same change in field, this constitutes a true implementation of the totally correlated model. By using refocusing π -pulses between gradients, it is also possible to dephase each spin separately, thereby implementing the uncorrelated model. At this time, however, we have collected and processed data only for the $\rho_{\text{A}}^1 = \mathbf{I}_z^1$ state with the totally correlated model.

Although it is possible to prepare the state $\mathbf{I}_z^1 \mathbf{E}_+^2 \mathbf{E}_+^3$ as noted above, we have chosen to illustrate the above analysis by preparing the states \mathbf{I}_z^1 , $2\mathbf{I}_z^1 \mathbf{I}_z^2$, $2\mathbf{I}_z^1 \mathbf{I}_z^3$ and $4\mathbf{I}_z^1 \mathbf{I}_z^2 \mathbf{I}_z^3$ in four separate experiments, each using sixteen different decoherence times t . Because the SQC and TQC contributing to $4\mathbf{I}_z^1 \mathbf{I}_z^2 \mathbf{I}_z^3$ refocused at different times, this further enabled us to follow their evolutions separately. The results of these experiments are plotted against the time t in Figure 4, along with the corresponding logarithmic fits. It may be seen that the sum of the data and of the fits thereto (also shown) do indeed exhibit a near-zero initial slope, in accord with the above calculations. Our published report [15] includes the results of further experiments (performed by E. Knill and R. Laffamme) with the natural and far more complicated decoherence processes that occur in solution.

These are more difficult to interpret, but are nevertheless consistent with the state preservation expected from error correction. Additional experiments and more detailed calculations are in progress.

While a method of inhibiting decoherence (T_2 relaxation) during NMR pulse sequences would be highly desirable, there are strong reasons to doubt that quantum error correction will be useful in this regard. First, the ancillae must be placed in a pseudo-pure state, which as we have shown above entails a loss of 50% of the signal for each “data” spin; this is more than is recovered by error correction. In addition, the ancillae must be returned to a pseudo-pure state uncorrelated with the state of the data spin(s), or else “fresh” ancillae in such a state must be continuously available, in order to inhibit decoherence over an appreciable period of time by the repeated correction of errors. Nevertheless, we feel that the basic idea underlying error correction of preparing multiple quantum coherences, allowing them to decohere, and then mixing them so as to determine their relative rates of relaxation, may be of considerable use in NMR studies of the statistics of molecular motion. This in turn is one of the most important applications of NMR spectroscopy. Conversely, whereas NMR spectroscopists have previously used their methods solely to unravel the secrets of naturally occurring systems, it now appears possible to use these same methods to engineer artificial systems in which the basic principles of quantum information processing, in particular the emergence of the classical world through decoherence [23], can be studied in unprecedented detail.

ACKNOWLEDGEMENTS

We thank E. Knill and R. Laflamme of Los Alamos National Labs for teaching us about quantum error correcting codes, and S. Braunstein and R. Jozsa for useful discussions on mixed-state correlation. This work was supported by the U. S. Army Research Office under grant number DAAG 55-97-1-0342 from the DARPA Ultrascale Computing Program.

References

1. Altmann, S. L. (1986): *Rotations, Quaternions and Double Groups*. Oxford Univ. Press, Oxford, U.K.
2. Aspect, A., Dalibard, J., Roger, G. (1982): Experimental tests of Bell’s inequalities using time-varying analyzers. *Phys. Rev. Lett.* **49**, 1804–1807.

3. Barenco, A., Bennett, C. H., Cleve, R., DiVincenzo, D. P., Margolus, N., Shor, P., Sleator, T., Smolin, J. A., and Weinfurter, H. (1995). Elementary gates for quantum computation. *Phys. Rev. A* **52**, 3457–3467.
4. Baylis, W. E., editor (1996): *Clifford (Geometric) Algebras, with Applications in Physics, Mathematics, and Engineering*. Birkhäuser, Boston, MA, Basel, C.H. and Berlin, D.
5. Biedenharn, L. C., Louck, J. D. (1981): *Angular Momentum in Quantum Physics*. Encyclopedia of Mathematics and Its Applications, Addison-Wesley Publishing Co., New York, NY.
6. Bloch, F. (1946): Nuclear induction. *Phys. Rev.* **70**, 460–474.
7. Blum, K. (1996): *Density Matrix Theory and Applications*. Plenum Pub. Corp. (2nd ed.).
8. Boulat, B., Rance, M. (1994): Algebraic formulation of the product operator formalism in the numerical simulation of the dynamic behavior of multispin systems. *Mol. Phys.* **83**, 1021–1039.
9. Boyer, M., Brassard, G., Hoyer, P., Tapp, A. (1998): Tight bounds on quantum searching. *Fort. Phys.* **46**, 493–505.
10. Branning, D. (1997): Does nature violate local realism? *Am. Sci.* **85**, 160–167.
11. Braunstein, S. L., Caves, C. M., Jozsa, R., Linden, N., Popescu, S. and Schack, R. (1998): Separability of very noisy mixed states and implications for NMR quantum computing. LANL preprint quant-ph/9811018.
12. Chuang, I. L., Gershenfeld, N., Kubinec, M. G., Leung, D. W. (1998): Bulk quantum computation with nuclear magnetic resonance: Theory and experiment. *Proc. R. Soc. Lond. A* **454**, 447–467.
13. Chuang, I. L., Vandersypen, L. M. K., Zhou, X., Leung, D. W., Lloyd, S. (1998): Experimental realization of a quantum algorithm. *Nature* **393**, 143–146.
14. Cory, D. G., Fahmy, A. F., Havel, T. F. (1997): Ensemble quantum computing by nuclear magnetic resonance spectroscopy. *Proc. Natl. Acad. Sci.* **94**, 1634–1639.
15. Cory, D. G., Maas, W., Price, M., Knill, E., Laflamme, R., Zurek, W. H., Havel, T. F., and Somaroo, S. S. (1998a). Experimental quantum error correction. *Phys. Rev. Lett.* **81**, 2152–2155.
16. Cory, D. G., Price, M. D., Havel, T. F. (1998b): Nuclear magnetic resonance spectroscopy: An experimentally accessible paradigm for quantum computing. *Physica D* **120**, 82–101.
17. Doran, C. J. L., Lasenby, A. N., Gull, S. F. (1993): States and operators in the spacetime algebra. *Found. Phys.* **23**, 1239–1264.

18. Doran, C. J. L., Lasenby, A. N., Gull, S. F., Somaroo, S. S., Challinor, A. D. (1996). Spacetime algebra and electron physics. In Hawkes, P., editor, *Advances in Imaging and Electron Physics*, pages 271–386. Academic Press, Englewood Cliffs, NJ.
19. Ernst, R. R., Bodenhausen, G., Wokaun, A. (1987): *Principles of Nuclear Magnetic Resonance in One and Two Dimensions*. Oxford Univ. Press, U.K.
20. Feynman, R. P., Vernon, F. L., Hellwarth, R. W. (1957): Geometrical representation of the Schrödinger equation for solving maser problems. *J. Appl. Phys.* **28**, 49–52.
21. Freeman, R. (1998): *Spin Choreography*. Oxford Univ. Press, Oxford, U.K.
22. Gershenfeld, N. A., Chuang, I. L. (1997): Bulk spin-resonance quantum computation. *Science* **275**, 350–356.
23. Giulini, D., Joos, E., Kiefer, C., Kupsch, J., Stamatescu, I., Zeh, H. D. (1996). *Decoherence and the Appearance of a Classical World in Quantum Theory*. Springer-Verlag.
24. Grover, L. K. (1997): Quantum mechanics helps in searching for a needle in a haystack. *Phys. Rev. Lett.* **79**, 325–328.
25. Gull, S. F., Lasenby, A. N., Doran, C. J. L. (1993): Imaginary numbers are not real. *Found. Phys.* **23**, 1175–1201.
26. Hardy, L. (1993): Nonlocality for two particles without inequalities for almost all entangled states. *Phys. Rev. Lett.* **71**, 1665–1668.
27. Havel, T. F. (1998): Distance geometry: Theory, algorithms and applications, in *The Encyclopedia of Computational Chemistry*. J. Wiley & Sons, Inc., New York, NY.
28. Hestenes, D. (1966): *Space-Time Algebra*. Gordon & Breach, New York, NY.
29. Hestenes, D. (1986): *New Foundations for Classical Mechanics*. D. Reidel Publishing Co., Dordrecht, NL.
30. Jaynes, E. T. (1957): Information theory and statistical mechanics, I & II. *Phys. Rev.* **106**, 620–650.
31. Jones, J. A., Hansen, R. H., Mosca, M. (1998): Quantum logic gates and nuclear magnetic resonance pulse sequences. *J. Magn. Reson.* **135**, 353–360.
32. Jones, J. A., Mosca, M., Hansen, R. H. (1998): Implementation of a quantum search algorithm on a quantum computer. *Nature* **393**, 344–346.
33. Jordan, T. F. (1994): Quantum mysteries explored. *Am. J. Phys.* **62**, 874–880.

34. Knill, E., Chuang, I., Laflamme, R. (1998): Effective pure states for bulk quantum computation. *Phys. Rev. A* **57**, 3348–3363.
35. Knill, E., Laflamme, R. (1997): Theory of quantum error-correcting codes. *Phys. Rev. A* **55**, 900–911.
36. Linden, N., Barjat, H., Freeman, R. (1998): An implementation of the Deutsch-Jozsa algorithm on a three-bit NMR quantum computer. *Chem. Phys. Lett.* **296**, 61–67.
37. Lloyd, S. (1998): Microscopic analogues of the Greenberger-Horne-Zeilinger experiment. *Phys. Rev. A*, 57:R1473–R1476.
38. Lounesto, P. (1997): *Clifford Algebras and Spinors*. London Math. Soc. Lect. Notes Ser., vol. 239, Cambridge Univ. Press, Cambridge, U.K.
39. Mermin, N. D. (1994): Quantum mysteries refined. *Am. J. Phys.* **62**, 880–887.
40. Munowitz, M. (1988): *Coherence and NMR*. J. Wiley & Sons, Inc., New York, NY.
41. Navon, G., Song, Y.-Q., Rööm, T., Appelt, S., Taylor, R. E., Pines, A. (1996). Enhancement of solution NMR and MRI with laser-polarized xenon. *Science* **271**, 1848–1851.
42. Nielsen, M. A., Knill, E., Laflamme, R. (1998): Complete quantum teleportation using nuclear magnetic resonance. *Nature* **396**, 52–55.
43. Peres, A. (1995): *Quantum Theory: Concepts and Methods*. Kluwer Academic Publishers, Dordrecht, NL.
44. Preskill, J. (1998): Unpublished lecture notes for a course on quantum computation (available from “<http://theory.caltech.edu/~preskill>”).
45. Sakurai, J. J. (1994): *Modern Quantum Mechanics*. Addison-Wesley Publishing Co., New York, NY.
46. Schulman, L. J., Vazirani, U. (1998): Scalable NMR quantum computation. LANL preprint quant-ph/9804060.
47. Slichter, C. P. (1990): *Principles of Magnetic Resonance (3rd. ed.)*. Springer-Verlag, Berlin, Germany.
48. Somaroo, S. S., Cory, D. G., Havel, T. F. (1998): Expressing the operations of quantum computing in multiparticle geometric algebra. *Phys. Lett. A* **240**, 1–7.
49. Sörensen, O. W. (1989): Polarization transfer experiments in high-resolution NMR spectroscopy. *Prog. NMR Spect.* **21**, 503–569.
50. Sörensen, O. W., Eich, G. W., Levitt, M. H., Bodenhausen, G., Ernst, R. R. (1983). Product operator formalism for the description of NMR pulse experiments. *Prog. NMR Spect.* **16**, 163–192.

51. Steane, A. M. (1998): Quantum computing. *Rep. Prog. Theor. Phys.* **61**, 117–173.
52. Stoff, M. E., Vega, A. J., Vaughan, R. W. (1977): Explicit demonstration of spinor character for a spin- $\frac{1}{2}$ nucleus via NMR interferometry. *Phys. Rev. A* **16**, 1521–1524.
53. Tang, C., Waugh, J. S. (1992): Dynamics of classical spins on a lattice: spin diffusion. *Phys. Rev. B* **45**, 748–754.
54. van de Ven, F. J. M., Hilbers, C. W. (1983): A simple formalism for the description of multiple-pulse experiments. Application to a weakly coupled two-spin ($I = \frac{1}{2}$) system. *J. Magn. Reson.* **54**, 512–520.
55. Warren, W. S. (1997): The usefulness of NMR quantum computing. *Science* **277**, 1688–1689. See also response by N. Gershenfeld and I. Chuang, pp. 1689–1690.
56. Williams, C. P., Clearwater, S. H. (1998): *Explorations in Quantum Computing*. Springer-Verlag, New York, NY.
57. Zhang, W., Cory, D. G. (1998): First direct measurement of the spin diffusion rate in a homogeneous solid. *Phys. Rev. Lett.* **80**, 1324–1327.